

Promising strategies employing nucleic acids as antimicrobial drugs

Luís Moreira,^{1,2} Nuno M. Guimarães,^{1,2} Rita S. Santos,^{1,2} Joana A. Loureiro,^{1,2} Maria C. Pereira,^{1,2} and Nuno F. Azevedo^{1,2}

¹LEPABE–Laboratory for Process Engineering, Environment, Biotechnology, and Energy, Faculty of Engineering, University of Porto, Rua Dr. Roberto Frias, 4200-465 Porto, Portugal; ²ALiCE–Associate Laboratory in Chemical Engineering, Faculty of Engineering, University of Porto, Rua Dr. Roberto Frias, 4200-465 Porto, Portugal

Antimicrobial resistance (AMR) is a growing concern because it causes microorganisms to develop resistance to drugs commonly used to treat infections. This results in increased difficulty in treating infections, leading to higher mortality rates and significant economic effects. Investing in new antimicrobial agents is, therefore, necessary to prevent and control AMR. Antimicrobial nucleic acids have arisen as potential key players in novel therapies for AMR infections. They have been designed to serve as antimicrobials and to act as adjuvants to conventional antibiotics or to inhibit virulent mechanisms. This new category of antimicrobial drugs consists of antisense oligonucleotides and oligomers, DNazymes, and transcription factor decoys, differing in terms of structure, target molecules, and mechanisms of action. They are synthesized using nucleic acid analogs to enhance their resistance to nucleases. Because bacterial envelopes are generally impermeable to oligonucleotides, delivery into the cytoplasm typically requires the assistance of nanocarriers, which can affect their therapeutic potency. Given that numerous factors contribute to the success of these antimicrobial drugs, this review aims to provide a summary of the key advancements in the use of oligonucleotides for treating bacterial infections. Their mechanisms of action and the impact of factors such as nucleic acid design, target sequence, and nanocarriers on the antimicrobial potency are discussed.

INTRODUCTION

Bacterial infectious diseases are becoming a serious threat to public health, mostly due to the emergence of antimicrobial resistance (AMR). The outlook is even bleaker as the appearance of multidrug resistance pathogens makes antimicrobial treatments increasingly ineffective in both third world and high-income countries.^{1–5} For instance, annually in the United States, over 2.8 million people fall ill due to AMR bacterial infections and 36,000 people succumb to the disease.⁶ In Europe, AMR causes approximately 33,000 deaths annually and imposes a substantial financial burden on European healthcare systems.⁷

Despite the increasing threat posed by AMR, the development of classical antibiotics is no longer deemed profitable by pharmaceutical companies.⁸ The lack of approval for new drugs, years of investment,

and millions of dollars spent have discouraged reinvestment in discovering antibiotics. Moreover, antibiotics are usually administered for a limited time, whereas treating chronic diseases requires patients to take medication for life, which is more economically attractive.^{8–10}

In contrast, researchers are exploring alternative approaches to classical antibiotics and have identified nucleic acids as potential novel antimicrobials or adjuvants to enhance the antimicrobial activity of these traditional drugs. Antimicrobial nucleic acids have been proposed to function either by disrupting molecular signaling pathways at the translational level or by interference with transcription.^{11,12} Independently of the inhibitory mechanism, antimicrobial nucleic acids prevent the target bacterium from producing proteins involved in essential metabolic processes, antibiotic resistance, or virulence mechanisms.^{13–15} Hence, selecting the appropriate target, such as the mRNA binding sequence or the transcription regulatory protein to be targeted, is a critical step in developing effective drugs.^{12,16–18}

There are still some challenges that need to be addressed to develop effective drugs. One such challenge is the sensitivity to nucleases, which makes natural nucleic acids unsuitable for administration in the human body. As a result, antimicrobial nucleic acids are typically designed using nucleic acid analogs, also known as nucleic acid mimics, which are resistant to enzymatic degradation (Figure 1).^{19–21} These nucleic acid analogs include noncharged backbones (e.g., peptide nucleic acids [PNAs], phosphorodiamidate morpholino oligomers [PMOs]), anionic oligonucleotides with sugar modifications (e.g., bridged nucleic acids [BNAs] or the homologous locked nucleic acid (LNA), 2'-O-methyl RNA [2'OMe]), as well as alternative internucleoside bonds (e.g., phosphorothioate (PS)). A comprehensive description of the structures and properties of these nucleic acid analogs can be found elsewhere.²²

<https://doi.org/10.1016/j.omtn.2024.102122>.

Correspondence: Luís Moreira, LEPABE–Laboratory for Process Engineering, Environment, Biotechnology, and Energy, Faculty of Engineering, University of Porto, Rua Dr. Roberto Frias, 4200-465 Porto, Portugal.

E-mail: luismoreira@fe.up.pt



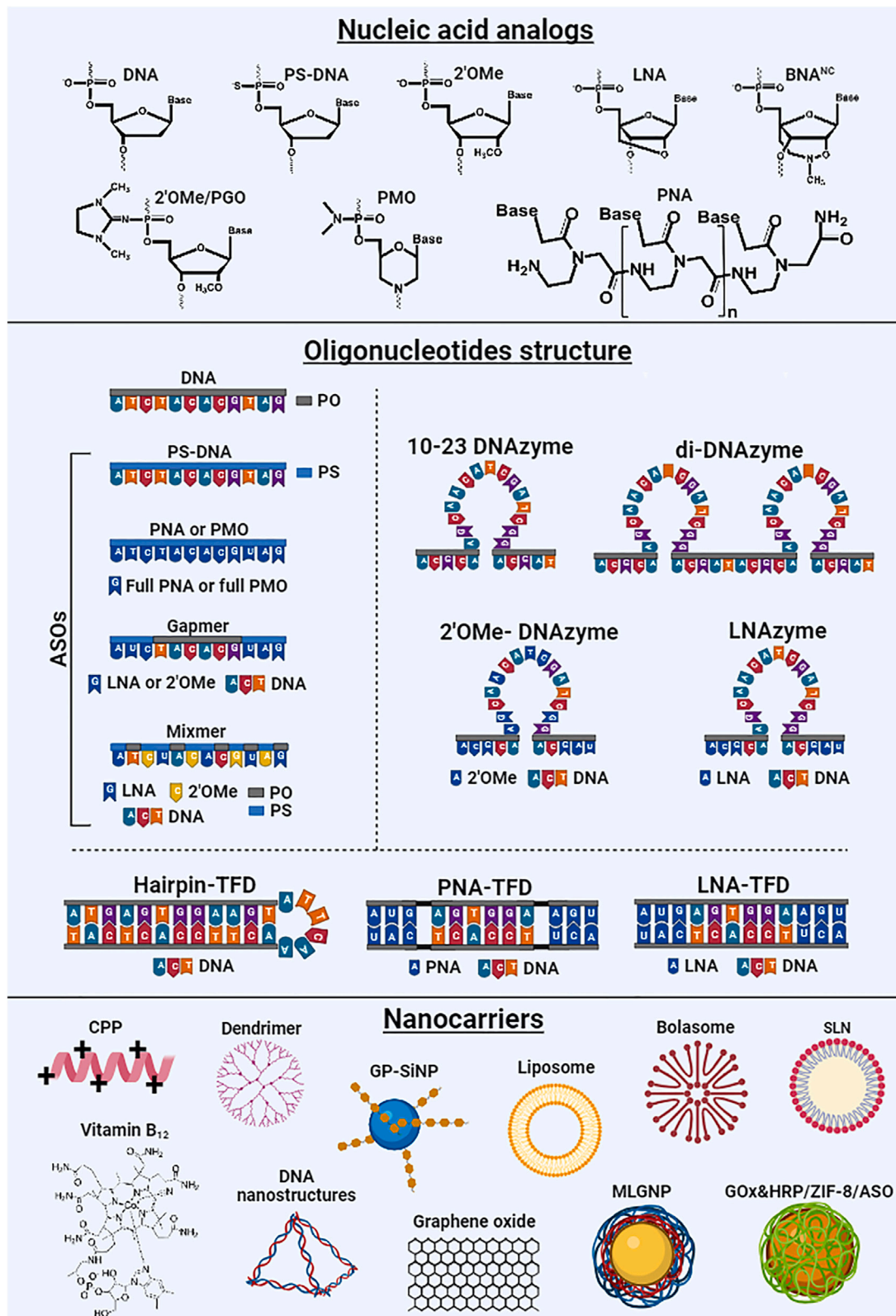


Figure 1. Structures of nucleic acid analogs, ASOs, TFDs, DNAzymes, and nanocarriers

Based on their mechanism of action, these nucleic acids are classified into antisense oligonucleotides and oligomers (ASOs), deoxyribozymes (DNAzymes), and transcription factor decoys (TFDs) (Figure 1). Although they have different structures, both ASOs and DNAzymes act at the translational level, inhibiting protein synthesis, whereas TFDs are intended to interfere with transcription, inhibiting mRNA synthesis, resulting in the downregulation of the target gene.

Regardless of their structure, these molecules need help crossing bacterial membranes effectively. Hence, nanocarriers are being explored to transport the nucleic acids in the human body and through multi-layered bacterial membranes (Figure 1). Examples of nanocarriers include cell-penetrating peptides (CPPs), liposomes, cationic bolaamphiphiles, and vitamin B₁₂ and DNA tetrahedrons, which differ in size, structure, properties, and other features.^{15,23–27} The properties of these nanocarriers also affect the potency of antimicrobial nucleic acids. Detailed information about the structures and properties of these nanocarriers has been published elsewhere.²²

The purpose of this review is to provide a comprehensive overview of potential antimicrobial nucleic acids–based strategies, along with fundamentals that underpin their design. A summary of the most frequently studied antimicrobial oligomers (CPP-conjugated PNA or PMO), alongside the latest advancements in the fields of antimicrobial nucleic acids design (mostly centered on anionic nucleic acid analogs) and intracellular delivery in bacteria (e.g., liposomes, cationic bolaamphiphiles, vitamin B₁₂ and DNA tetrahedrons), will be presented. This is succeeded by a critical analysis of the most promising nucleic acids–based treatments for bacterial infections.

ASOs

In 1991, Rahman and coworkers²⁸ introduced an innovative approach to combat bacterial infections using ASOs aimed at targeting the 16S rRNA in *Escherichia coli*. This study has demonstrated an alternative strategy for the development of novel antimicrobial drugs.

Currently, ASOs are primarily engineered to block the mRNA translation of both essential and nonessential genes. Several essential genes such as the *gyrA*, *ftsZ*, and *acpP* have already been recognized as potential targets for antimicrobial ASOs.^{11,16,18,24,29–35} Despite being prevalent in a wide range of both Gram-negative and Gram-positive pathogens,^{11,16–18,24,26,29–42} the presence of mutations in these genes can pose challenges in designing broad-spectrum ASOs. However, they still serve as suitable targets for narrow-spectrum ASOs.²³ Moreover, ASOs can target genes that, although not essential for bacterial survival, provide adaptive advantages, such as virulence genes involved in biofilm formation.^{13,43} By targeting antibiotic-resistance genes, ASOs can also enhance the effectiveness of most broad-spectrum antibiotics.^{15,44–51} Table 1 shows a list of potential target genes for antimicrobial nucleic acids.

Regardless of the targeted mRNA, ASOs must identify a specific sequence and inhibit the translation of a functional protein. To vali-

date the specificity of ASOs, the experiments routinely incorporate mismatched and scrambled nucleic acids, along with controls involving unloaded nanocarriers. In bacteria, the antisense inhibition of mRNA translation occurs via either steric blocking of RNA sequences or cleavage of the mRNA through recruitment of RNase H, depending on the structure of the ASOs (Figures 1 and 2).¹¹ The prediction of the antisense mechanism typically relies on the RNase H assay, which assesses the extent to which ASO/RNA heteroduplexes are cleaved by RNase H.^{52,53}

MECHANISM OF INHIBITION OF mRNA TRANSLATION VIA ASOs: RNase H-MEDIATED CLEAVAGE

The recruitment of RNase H activity (Figure 2) implies the formation of an ASO/RNA heteroduplex mimicking the DNA/RNA heteroduplex geometry. In contrast to DNA/DNA and RNA/RNA duplexes, which adopt B-form and A-form structures, respectively, the DNA/RNA heteroduplexes assume an intermediate form characterized by a O4'-endo conformation.^{54,55} This geometric arrangement may elucidate how RNase H discerns RNA duplexes from DNA/RNA hybrids, ultimately leading to the cleavage of the RNA strand involved in heteroduplex structures.⁵⁵ However, considering the need for biological stability to create effective drugs, some level of modification is desirable. As such, oligonucleotides containing PS-modified internucleoside linkages are favored over natural nucleotides (DNA) containing phosphodiester (PO) linkages to design RNase H-dependent ASOs (Figure 1).⁵⁶ The second generation of ASOs are called gapmers and aim to improve the stability and specificity of these oligonucleotides while preserving RNase H activity (Figure 1).^{57,58} Gapmers consist of a central DNA or PS/DNA sequence to recruit RNase H activity, flanked by regions composed of nucleotides with modified sugars such as 2'OMe or LNA to increase the target affinity and resistance to nucleases. Kurreck et al.⁵⁹ evaluated various gapmer designs and found that a gap of 6 and 7 DNA residues in 2'OMe or LNA-modified gapmers, respectively, was required for the complete activation of RNase H. Furthermore, the RNase H activity was correlated with the affinity of the flanking regions to the target RNA, with nuclease activity decreasing in the order of LNA > 2'OMe > DNA > PS/DNA, with LNA flanks providing the strongest inhibition.⁵¹ However, the excessive affinity of LNA-gapmers has also been associated with hepatotoxicity due to RNase H-mediated cleavage of off-target RNAs.^{60,61} For 16-mer LNA-gapmers, a melting temperature below 55°C was found to significantly improve specificity and thus reduce cytotoxicity.⁶²

MECHANISM OF INHIBITION OF mRNA TRANSLATION VIA ASOs: STERIC BLOCKING

Steric blocking ASOs are designed to form stable ASO/RNA heteroduplexes that prevent translation by hindering ribosomal maturation or polypeptide elongation (Figure 2). Therefore, these ASOs usually bind to regions of regulatory sequences in mRNA, such as the start codon region (translation initiation site)^{16,24,35} or the Shine-Dalgarno sequence (ribosomal-binding site),¹⁸ where initiation of the translation occurs.⁵⁶ Moreover, the lack of secondary structures

Table 1. Potential target genes for antimicrobial oligonucleotides

Gene	Gene classification	Encoded protein and/or function	Target bacteria	Reference
<i>gyrA</i>	Essential	DNA gyrase subunit A	<i>Staphylococcus</i> spp.; <i>Streptococcus</i> spp.; <i>K. pneumoniae</i> ; <i>Acinetobacter</i> spp.; <i>Brucella</i> spp.; <i>A. baumannii</i> ; <i>B. anthracis</i> ; <i>S. pyogenes</i> ; <i>S. pneumoniae</i> ; <i>S. aureus</i>	Panchal et al. ¹⁸ , Geller et al. ²⁴ , Nekhotiaeva et al. ²⁹ , Patenge et al. ³⁰ , Kurupati et al. ³¹ , Wang et al. ³² , Rajasekaran et al. ³³ , Barkowsky et al. ³⁶ , and Barkowsky et al. ¹⁰²
<i>ompA</i>		Outer membrane protein A	<i>K. pneumoniae</i>	Kurupati et al. ³¹
<i>ftsZ</i>		Filament temperature-sensitive protein Z Cell division protein ftsZ	<i>Staphylococcus</i> spp.; <i>Streptococcus</i> spp.; <i>K. pneumoniae</i> ; <i>Acinetobacter</i> spp.; <i>Brucella</i> spp.; <i>A. baumannii</i> ; <i>B. anthracis</i> ; <i>P. aeruginosa</i>	Liang et al. ¹⁷ , Panchal et al. ¹⁸ , Geller et al. ²⁴ , Nekhotiaeva et al. ²⁹ , Patenge et al. ³⁰ , Kurupati et al. ³¹ , Wang et al. ³² , Rajasekaran et al. ³³ , Ghosal and Nielsen ³⁵ , Zhang et al. ³⁷ , Meng et al. ³⁸ , Long et al. ¹¹⁹ , and Zhang et al. ¹³⁰
<i>acpP</i>		Acyl carrier protein involved in fatty acid synthesis	<i>E. coli</i> ; <i>Pseudomonas</i> spp.; <i>Brucella</i> spp.; <i>B. cepacia</i> ; <i>Salmonella enterica</i> Serovar Typhimurium; <i>A. lwoffii</i> ; <i>A. baumannii</i> ; <i>B. anthracis</i> ; <i>K. pneumoniae</i>	Bai and Luo ¹¹ , Greenberg et al. ¹⁶ , Panchal et al. ¹⁸ , Geller et al. ²⁴ , Równicki et al. ²⁶ , Rajasekaran et al. ³³ , Good et al. ³⁴ , Ghosal and Nielsen ³⁵ , Yavari et al. ³⁹ , Tilley et al. ⁴⁰ , Mellbye et al. ⁴¹ , Perche et al. ⁴² , Iubatti et al. ¹⁰⁸ , Liu et al. ¹¹⁶ , and Chen et al. ¹²⁴
<i>rpoA</i>		RNA polymerase subunit α	<i>L. monocytogenes</i>	Alajjlouni and Selem ⁸³ and Abushahba et al. ⁹⁵
<i>rpoB</i>		RNA polymerase subunit β	<i>C. difficile</i>	Hegarty et al. ⁸⁵
<i>rpoD</i>		Transcription initiation factor	<i>L. monocytogenes</i> ; MRSA <i>E. coli</i> ; <i>S. enterica</i> ; <i>K. pneumoniae</i> ; <i>Shigella flexneri</i>	Bai et al. ²³ , Bai et al. ⁸¹ , Alajjlouni and Selem ⁸³
<i>polA</i>		DNA polymerase I	<i>B. suis</i>	Rajasekaran et al. ³³
<i>asd</i>		Aspartate- β -semialdehyde dehydrogenase; cell envelope synthesis	<i>B. suis</i>	Rajasekaran et al. ³³
<i>dnaG</i>		DNA primase	<i>B. suis</i>	Rajasekaran et al. ³³
<i>fmhB</i>		Cell wall synthesis	<i>S. aureus</i>	Nekhotiaeva et al. ²⁹
<i>inhA</i>		Mycolic acid biosynthesis	<i>M. smegmatis</i>	Kulyté et al. ⁹⁷
<i>ald</i>		Alanine dehydrogenase	<i>M. smegmatis</i>	Skvortsova et al. ⁵²
<i>fbpA, fbpB, fbpC</i>		Antigens 85A, 85B, 85C (mycolyl- transferase activity); cell wall synthesis	<i>M. tuberculosis</i>	Harth et al. ¹²⁵
<i>sigH</i>		RNA polymerase sigma-H factor; transition from exponential growth to stationary phase and initiation of sporulation	<i>C. difficile</i>	Marín-Menéndez et al. ²⁵
<i>Fur</i>		FUR transcription factor; import of iron	<i>E. coli</i> K12	González-Paredes et al. ¹³⁴
<i>fmhB</i>		Synthesis of peptidoglycan	MRSA	Liu et al. ¹¹⁶

(Continued on next page)

Table 1. Continued

Gene	Gene classification	Encoded protein and/or function	Target bacteria	Reference
THI-box present in several operons		TPP riboswitch	<i>L. monocytogenes</i>	Traykovska et al. ¹²²
S-box operon		SAM-I riboswitch	<i>L. monocytogenes</i> ; <i>S. aureus</i>	Traykovska and Penchovsky ¹²³
<i>MotA</i>	Virulence	Cytoplasmic membrane protein; bacterial adhesion and biofilm formation	<i>P. aeruginosa</i>	Hu et al. ¹³
<i>efaA</i>		<i>Enterococcus faecalis</i> antigen A; bacterial adhesion and biofilm formation	<i>E. faecalis</i>	Narenji et al. ⁴³
<i>gtfBCD, gbpB, ftf</i>		Adhesion-associated protein; biofilm formation	<i>S. mutans</i>	Zhang et al. ²⁷
<i>icl</i>		Isocitrate lyase; essential for <i>M. tuberculosis</i> survival in macrophages	<i>Mycobacterium tuberculosis</i>	Li et al. ¹⁴⁸
<i>agrA</i>		Accessory gene regulator; quorum sensing system in MRSA responsible for regulating the expression of virulence genes, including toxins and degradative exoenzymes	MRSA	Da et al. ¹²¹
<i>YycFG</i> (or <i>WalRK</i> or <i>VicRK</i>)		Two-component regulatory system; control cell wall metabolism, membrane composition; biofilm formation	<i>S. aureus</i>	Wu et al. ¹²⁶
<i>mar</i> operon	Antibiotic resistance	Reduce traffic of tetracyclines through the outer membrane; reduce quinolone-induced DNA damage	<i>Enterobacteriaceae</i>	White et al. ⁴⁶ and Sharma et al. ⁴⁷
CmeABC operon		CmeABC multidrug efflux pump	<i>Campylobacter jejuni</i>	Oh et al. ⁴⁸
<i>mexAB-oprM</i> operon		Multidrug efflux pump	<i>P. aeruginosa</i>	Wang et al. ⁴⁹
<i>acrB</i>		AcrAB-TolC efflux pump; resistance to fluoroquinolones	<i>E. coli</i>	Meng et al. ⁵⁰
<i>mecA</i>		PBP2a; transpeptidase with low binding affinity to β -lactams	MRSA	Meng et al. ¹⁵ , Goh et al. ⁵¹ , and Beha et al. ¹²⁹
<i>mecR1</i>		β -Lactam-sensing transmembrane signaling protein; <i>mecA</i> gene regulator	MRSA	Ran et al. ¹⁵⁴
<i>bla</i> _{CTX-M-group 1}		β -Lactamase CTX-M-group 1	<i>E. coli</i>	Readman et al. ¹¹²
<i>aac</i> (ϵ')- <i>Ib</i>		Aminoglycoside-modifying enzymes; amikacin resistance	<i>A. baumannii</i>	Lopez et al. ⁹⁴
<i>WalR</i>		WalR transcription regulator; control cell wall metabolism, membrane composition, and resistance to vancomycin	MRSA	Hibbitts et al. ⁸⁷
PBP2a, penicillin-binding protein 2a.				

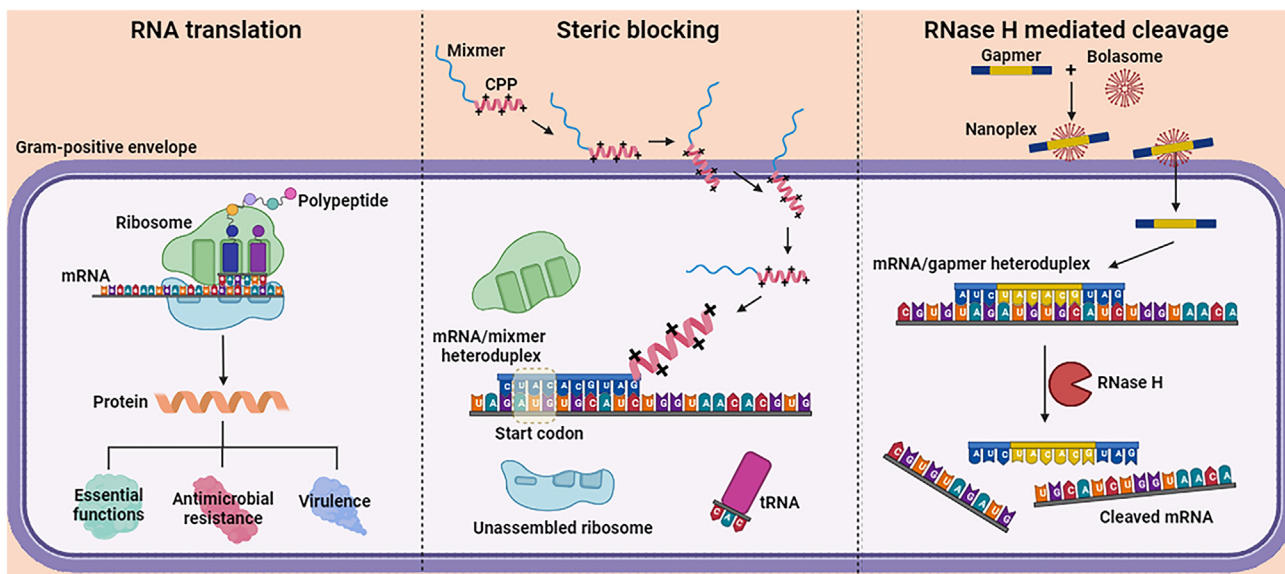


Figure 2. Inhibition of the mRNA translation through the steric blocking or RNase H-mediated cleavage mechanisms

In the absence of ASOs, the mRNA is translated into a protein responsible for essential functions, antibiotic resistance, or virulence mechanisms in bacterial cells. The binding of steric blocking ASOs to a specific mRNA sequence hinders the formation of the ribosomal apparatus or the translation of a complete and functional protein, thus exerting antimicrobial activity or inhibiting the antibiotic resistance or virulence mechanisms. Recruitment of the RNase H activity cleaves the ASO/RNA heteroduplexes, hindering the mRNA translation. (This figure was created with [BioRender.com](#).)

in these regions makes them accessible targets for small ASOs binding. As a result, the inhibition is highly efficient.^{11,63}

The steric blocking mechanism demands the formation of an ASO/RNA heteroduplex that is resistant to RNase H degradation.^{19,64} This can be achieved by using PMO, because PMO/RNA heteroduplexes do not serve as substrates for RNase H activity.⁶⁵ In addition, PMO is considered safe, having been approved by the US Food and Drug Administration for treating Duchenne muscular dystrophy in the form of the nucleic acid drug eteplirsen (Exondys 51).⁶⁶ Like PMO, PNA does not recruit RNase H. In fact, PNA/RNA heteroduplexes adopt a conformation resembling that of A-form RNA duplexes.⁶⁷ However, PNA oligomers require the conjugation of hydrophilic molecules due to concerns related to water solubility.^{21,68–70} PMO and PNA oligomers are synthesized exclusively using PMO and PNA monomers, respectively (Figure 1). This is due to the incompatibility of their synthesis with DNA, RNA, or other nucleic acid analogs. In contrast, anionic nucleic acid analogs containing 2'-substituents, such as 2'OMe and LNA (or BNA), can be incorporated into the same oligonucleotide (forming mixmers) along with natural nucleic acids (DNA and RNA), as well as PO and PS internucleoside linkages (Figure 1).^{59,71–74} 2'OMe and LNA adopt the canonical (C3'-endo) A-form RNA conformation, being invisible to RNase H.^{54,75,76} However, 2'OMe can pose toxicity concerns due to nonspecific binding to proteins.⁷⁷ In contrast, LNA are less prone to protein binding,⁷⁸ and additionally exhibit superior affinity and specificity to RNA.^{53,79,80} It is worth noting that an excess of affinity in LNA mixmers is likely to result in the same toxicity issues found in LNA-containing gapmers.^{60,61}

INFLUENCE OF THE TARGET SEQUENCE IN ASOS INHIBITORY POTENCY

After overcoming the delivery barrier, the susceptibility of the target sequence to antisense inhibition dictates the potency of ASOs. In fact, even when targeting the start codon and Shine-Dalgarno regions, selecting the most sensitive positions is crucial to enhance the inhibition of gene expression through steric blocking. For instance, Geller et al.²⁴ tested PMO targeting *acpP* mRNA in *Acinetobacter* at the positions [−16; −6] and [1; 11] (numbering from the first base of the start codon) and achieved higher antimicrobial activity with the PMO sequence overlapping the start codon. Greenberg et al.¹⁶ also showed that the CPP-PMO conjugates targeting the start codon ([−5; 6]) of *acpP* mRNA in *Burkholderia* were more potent than those targeting a near-downstream sequence ([4; 14]). A similar observation was made in *Pseudomonas aeruginosa* using PNA.³⁵ When targeting *ftsZ* mRNA, the lowest minimum inhibitory concentration (MIC) was achieved by ASOs targeting downstream positions, partially including the start codon (1 or 2 nucleotide residues downstream) or with no overlap ([4; 13]). These results confirm that the hybridization of ASOs near or overlapping the start codon is an effective approach for downregulating gene expression. However, there are exceptions to this rule, as demonstrated by Panchal and collaborators.¹⁸ They found that in *Bacillus anthracis*, PMOs complementary to the start codon of the *acpP* mRNA or to a sequence near it ([−9; 2] and [4; 14], respectively) were less effective than ASOs targeting a distant upstream position ([−17; −7]). Similarly, ASOs targeting the [−16; −6] position of the *gyrA* mRNA were more potent than their counterparts targeting a

near-start codon position ([4; 14]). The authors suggested that overlapping with the apparent ribosome binding site (7–9 bases upstream from the start codon) was the most likely reason behind the higher antimicrobial activity of ASOs targeting upstream positions.

In addition to the translation initiation region, binding ASOs to a specific interior region within the mRNA sequence can result in a high inhibitory effect. Liang et al.¹⁷ used folding software to predict the secondary structure of *ftsZ* mRNA and selected 10 open sites within the stem-loop regions. They designed several ASOs, which were screened for binding efficiency using dot-blot hybridization. After selecting the [309; 323] position through screening, they designed a PNA oligomer to target it. To compare the inhibitory potency, this PNA-ASO was tested against another one targeting the start codon ([–9; 3]), and both PNA-ASOs were conjugated to the (RXR)₄XB peptide (R is arginine; X is 6-aminohexanoic acid; B is β-alanine). The two conjugates inhibited methicillin-resistant *Staphylococcus aureus* (MRSA) growth at concentrations of 30 and 40 μM, respectively, with the conjugate targeting the [309; 323] position showing higher effectiveness (lower concentration required). Interestingly, the most potent conjugate, targeting the [309; 323] position of *ftsZ* mRNA, was designed with a longer sequence (15-mer) than the counterpart targeting the start codon region (12-mer). This finding suggests that long PNA sequences can be as effective as short ones targeting the translational regulatory sequences if highly sensitive binding sites downstream of the start codon are targeted. Bai et al.⁸¹ also noted that the *rpoD* mRNA, which encodes the primary sigma 70 factor of RNA polymerase in MRSA, contains an internal region with high sensitivity to antisense inhibition. In this case, however, the most potent PNA matched a structured region of the mRNA, which is typically less sensitive to antisense inhibition. Despite the many alternative binding sites generated by these approaches, designing an effective ASO targeting these regions can be more challenging and time-consuming than simply targeting the start codon and Shine-Dalgarno regions.

INTRACELLULAR DELIVERY OF ASOs IN BACTERIA

There is a consensus that the major limitation of ASOs as antimicrobial drugs is delivering them to the bacterial cytosol in a sufficient amount to inhibit gene expression.^{15–18,23–25,27,31,38,41,51,82–87} Unlike classical antibiotics that can pass through bacterial envelopes, partially due to their small molecular weight, ASOs are comparatively larger molecules and thus face obstacles in achieving the same feat. A few studies have highlighted lipopolysaccharide as a significant barrier to the penetration of PNA in *Escherichia coli*.^{88,89} In Gram-positive bacteria, the thickness of the peptidoglycan layer also plays a crucial role in the diffusion of PNA through the bacterial wall, with increased thickness leading to greater restrictions in diffusion.⁹⁰ Concerning the anionic oligonucleotides, they still need to overcome the electrostatic repulsion caused by the negatively charged surface of both Gram-negative and Gram-positive bacteria.^{72,91} Moreover, their size makes it challenging for them to passively diffuse through the outer membrane of the Gram-negative bacteria.⁹²

Studies on determining the optimal size of antisense oligomers have indicated that 10- to 12-mer oligomers are more efficiently internalized into bacteria and exhibit a greater inhibitory effect than either longer or shorter oligomer strands.^{34,35,93} Nonetheless, these studies mostly used uncharged ASO-CPP conjugates targeting the start codon region, which may not reflect the behavior of other nucleic acid analogs and delivery systems. In fact, the lengths of other ASOs have been successfully delivered. For example, LNA and aminoBNA^{NC} ASOs with lengths of 21- and 15-mers, respectively, have been shown to cross the bacterial envelope with the assistance of CPPs.^{38,94} In addition, anionic ASOs with lengths ranging from 17- to 25-mers have been successfully delivered into bacteria using lipid particles and DNA tetrahedrons.^{15,27,49,50,85} These results suggest that the optimal length of ASOs must be determined based on the type of nucleic acid analogs and nanocarrier used to achieve the maximum inhibitory activity.

In this regard, research into nanocarriers within the context of nucleic acids delivery into bacteria assumes a crucial role in the advancement of this therapeutic technology. However, due to the diversity of target genes and bacteria used in these studies, as well as a lack of *in vivo* studies demonstrating the efficacy of ASO-nanocarrier constructs, a direct comparison of the nanocarrier performance is quite difficult. Nevertheless, a clear distinction exists between the types of nanocarriers used for intracellular delivery in bacteria, depending on whether the ASOs are charge neutral or anionic. Although charge-neutral ASOs are primarily linked to CPPs, anionic ASOs exhibit greater variability in terms of the nanocarrier class used.

INTRACELLULAR DELIVERY OF CHARGE-NEUTRAL ASOs

Of the nucleic acid analogs, PNA and PMO are the ones mostly studied as antimicrobial ASOs in animal models bearing bacterial infections (Figure 1). These oligomers are often conjugated to CPPs, resulting in MICs in the range of 0.2–62.5 μM for Gram-negative bacteria and 0.1–80 μM for Gram-positive species (Table 2). In both instances, the MICs vary greatly, reflecting the different performance of CPPs across different bacterial species as well as the target sequence. A widely used CPP is the (KFF)₃K (K-lysine; F-phenylalanine) peptide conjugated to PNA or PMO. These constructs have shown MICs ranging from 0.2 to 12.5 μM against pathogens such as *E. coli*, *Salmonella typhimurium*, *Klebsiella pneumoniae*, *Listeria monocytogenes*, and *S. aureus*.^{26,29–31,33,34,38–40,51,81–83,95–97} In mouse models, the effectiveness of (KFF)₃K conjugates as therapeutic agents was also demonstrated. A dose of 3 mg/kg of (KFF)₃K-PNA was sufficient to improve the survival of mice infected with *E. coli*. Despite the promising outcomes, the prospects of (KFF)₃K-PNA conjugates as novel antimicrobials are bleak because mutant strains (e.g., mutations in the *sbmA* gene encoding an inner membrane peptide transporter that recognizes and transports PNA) exhibiting resistance to these conjugates have already been identified.^{39,98} In addition, the potential toxic effects of the (KFF)₃K peptide should be considered before its further development as an antimicrobial drug.^{99,100} Hemolytic activity was also reported at 40 μg/mL for this CPP.¹⁰¹

Table 2. Composition, *in vitro* and *in vivo* inhibitory concentrations of the antimicrobial oligonucleotides, and their bacterial targets

Carrier + oligonucleotide	<i>In vitro</i> antimicrobial activity	<i>In vivo</i> antimicrobial activity	Bacteria	Reference
(KFF) ₃ K-PNA	MIC: 0.2 μM	N.A.	<i>E. coli</i> K12	Good et al. ³⁴
	MIC: 4 μM Growth inhibition: 40 μM	Bacteremia in BALB/c mice: 500 nmol	<i>E. coli</i> K12	Tan et al. ⁸²
	Growth inhibition: 5 μM	N.A.	<i>E. coli</i> K12	Równicki et al. ²⁶
	MIC: 2 μM Growth inhibition: 20–40 μM	N.A.	<i>K. pneumoniae</i>	Kurupati et al. ³¹
	Growth inhibition: 12.5 μM Intracellular inhibition: 30 μM	N.A.	<i>B. suis</i>	Rajasekaran et al. ³³
	MIC: 5 μM Intracellular MIC: 15 μM	<i>C. elegans</i> model: 15–30 μM	<i>L. monocytogenes</i>	Alajlouni and Seleem ⁸³
	MIC ₅₀ : 32 μM Intracellular MIC: 8 μM	<i>C. elegans</i> model: 16–32 μM	<i>L. monocytogenes</i>	Abushahba et al. ⁹⁵
	MIC: 1.6 μM	N.A.	<i>S. pyogenes</i>	Patenge et al. ³⁰
	Growth inhibition: 2.5–5 μM	N.A.	MRSA	Goh et al. ⁵¹
	MIC: 12.5 μM	N.A.	MRSA	Bai et al. ⁸¹
	MIC: 2 μM Growth inhibition: 10 μM	N.A.	<i>S. aureus</i>	Nekhotiaeva et al. ²⁹
	MIC: 2 μM	N.A.	<i>M. smegmatis</i>	Kulyté et al. ⁹⁷
	MIC: 2 μM	N.A.	<i>E. coli</i>	Yavari et al. ³⁹
(KFF) ₃ K-PNA (D-form peptide)	MIC: 2–4 μM	N.A.	<i>E. coli</i>	Yavari et al. ³⁹
(RXR) ₄ XB-PNA	MIC: 1–2 μM	N.A.	<i>P. aeruginosa</i>	Ghosal and Nielsen ³⁵
	MIC: 2–4 μM	N.A.	<i>P. aeruginosa</i>	Maekawa et al. ⁸⁴
	MIC: 5 μM	Sepsis BALB/c mice model: 10 mg/kg	ESBLs- <i>E. coli</i>	Bai et al. ²³
	MIC: 2.5 μM	Sepsis BALB/c mice model: 10 mg/kg	MDR- <i>S. flexneri</i>	Bai et al. ²³
	MIC: 30 μM	N.A.	ESBLs- <i>K. pneumoniae</i>	Bai et al. ²³
	MIC: 12.5 μM	N.A.	MDR- <i>S. enterica</i>	Bai et al. ²³
	MIC: 62.5 μM	<i>G. mellonella</i> model: 4 nmol	<i>S. pyogenes</i>	Barkowsky et al. ³⁶
	MIC ₅₀ : 1 μM Intracellular MIC <2 μM	<i>C. elegans</i> model: 16–32 μM	<i>L. monocytogenes</i>	Abushahba et al. ⁹⁵
	Growth inhibition: 30 μM	N.A.	MRSA	Liang et al. ¹⁷
	IC ₅₀ : 0.63 μM	<i>G. mellonella</i> model: 10 nmol	<i>S. pneumoniae</i> strains TIGR4, D39, 19F	Barkowsky et al. ¹⁰²
(RX) ₆ -PNA	MIC: 2 μM	N.A.	<i>P. aeruginosa</i>	Ghosal and Nielsen ³⁵
(RFR) ₄ XB-PNA	MIC ₅₀ : 4 μM Intracellular MIC: 2 μM	<i>C. elegans</i> model: 16–32 μM	<i>L. monocytogenes</i>	Abushahba et al. ⁹⁵
TAT-PNA	MIC: 15.6 μM	<i>G. mellonella</i> model: 4 nmol	<i>S. pyogenes</i>	Barkowsky et al. ³⁶
	MIC ₅₀ : 2 μM Intracellular MIC: 2 μM	<i>C. elegans</i> model: 16–32 μM	<i>L. monocytogenes</i>	Abushahba et al. ⁹⁵

(Continued on next page)

Table 2. Continued

Carrier + oligonucleotide	<i>In vitro</i> antimicrobial activity	<i>In vivo</i> antimicrobial activity	Bacteria	Reference
B12-(CH ₂) ₆ -PNA B12-SS-PNA	Growth inhibition: 5 μM	N.A.	<i>E. coli</i> K12	Równicki et al. ²⁶
DNA tetrahedron-PNA	Growth inhibition: 40 μM IC ₅₀ : 0.750 μM	N.A.	<i>E. coli</i> MRSA	Readman et al. ¹¹² Zhang et al. ³⁷
Dendron-PNA	MIC: 0.5 μM MIC: 8 μM	Neutropenic murine peritonitis model: 20 mg/kg N.A.	<i>E. coli</i> <i>K. pneumoniae</i>	Iubatti et al. ¹⁰⁸
GP-SINPs-ASPNA	MIC: 0.8 μM	Keratitis and endophthalmitis mouse models: 1 μM (20 μL)	<i>E. coli</i> ; MRSA	Liu et al. ¹¹⁶
(KFF) ₃ K-PMO	IC ₅₀ : 9.5 μM IC ₅₀ : 9.5 μM Luciferase inhibition: 20 μM	N.A.	<i>E. coli</i> <i>S. enterica</i> <i>E. coli</i>	Tilley et al. ⁴⁰ Geller et al. ⁹⁶
(RXR) ₄ XB-PMO	MIC: 0.1–2 μM MIC: 2–8 μM MIC: 1.25 μM MIC: >40 μM MIC: 80 μM	Murine pulmonary infection model: 0.25–5 mg/kg Mouse peritonitis: 1.5 mg/kg N.A. N.A.	<i>A. lwoffii</i> ; <i>A. baumannii</i> <i>E. coli</i> <i>B. cepacia</i> <i>B. anthracis</i>	Geller et al. ²⁴ Mellbye et al. ⁴¹ Greenberg et al. ¹⁶ Panchal et al. ¹⁸
(RFF) ₃ XB-PMO	IC ₅₀ : 3.6–5.2 μM IC ₅₀ : 0.5 μM MIC: 0.5–1 μM MIC: 4–8 μM MIC: 1.25–5 μM	N.A. N.A. Virulent Ames <i>B. anthracis</i> - infected C57BL/6 mice: 5 mg/kg	<i>E. coli</i> <i>S. enterica</i> <i>A. lwoffii</i> <i>A. baumannii</i> <i>B. anthracis</i>	Tilley et al. ⁴⁰ Geller et al. ²⁴ Panchal et al. ¹⁸
	MIC: 2.5–10 μM	CGD mice infected with <i>Burkholderia multivorans</i> : 200 μg	<i>B. cepacia</i>	Greenberg et al. ¹⁶
	MIC: 2.5 μM	N.A.	<i>E. coli</i>	Mellbye et al. ⁴¹
(rff) ₃ xb-PMO (D-form peptide)	MIC: 5 μM	N.A.	<i>E. coli</i>	Mellbye et al. ⁴¹
(RFR) ₄ XB-PMO	MIC: 0.625 μM	Mouse peritonitis: 15 mg/kg	<i>E. coli</i>	Mellbye et al. ⁴¹
(RX) ₆ -PMO	MIC: 1.25 μM	Mouse peritonitis: 5 mg/kg	<i>E. coli</i>	Mellbye et al. ⁴¹
DPPC/DMPG (molar ratio: 10:1) loaded with PS/DNA	<i>lacZ</i> inhibition: 10–25 μM	N.A.	<i>E. coli</i> CSH36	Fillion et al. ¹¹⁷
DSPC/cardiolipin liposomes (molar ratio: 58:42) loaded with PS/DNA-PEI complexes (PEI/ASO weight ratio: 6)	Growth inhibition: 1 μM	N.A.	<i>E. coli</i> ; <i>P. aeruginosa</i>	Perche et al. ⁴²
EPC/DMPG/PEG2000-DSPE liposomes (molar ratio: 14:0.9:1) loaded with PS/DNA-PEI complexes (N/P ratio: 8)	MIC: 3 μg/mL (0.5 μM) Resistance gene inhibition: 100 μg/mL (17.4 μM)	N.A.	MDR- <i>P. aeruginosa</i>	Wang et al. ⁴⁹

(Continued on next page)

Table 2. Continued

Carrier + oligonucleotide	<i>In vitro</i> antimicrobial activity	<i>In vivo</i> antimicrobial activity	Bacteria	Reference
	MIC: 3 µg/mL (0.5 µM) Resistance gene inhibition: 100 µg/mL (17.4 µM)	N.A.	Fluoroquinolone-resistant <i>E. coli</i>	Meng et al. ⁵⁰
	MIC: 0.7 µM Resistance gene inhibition: 18 µM	Sepsis mice model: 5–10 mg/kg	MRSA	Meng et al. ¹⁵
Micelles of lipid moiety-PS/DNA	Resistance gene inhibition: 5 µM (no antisense activity was observed by qRT-PCR and western blotting)	N.A.	ESBLs- <i>E. coli</i>	Kauss et al. ¹¹⁸
Cationic bolaamphiphile nanoplexes loaded with 2'OMe- PS/DNA-2'OMe gapmer	MIC: 0.2–0.8 µM	N.A.	<i>C. difficile</i>	Hegarty et al. ⁸⁵
DNA tetrahedron–2'OMe/PS/DNA mixmer	Biofilm inhibition: 0.750 µM	N.A.	<i>S. mutans</i>	Zhang et al. ²⁷
6HB loaded PS/DNA	Growth inhibition (57.6%): 0.6 µM	N.A.	<i>S. aureus</i>	Long et al. ¹¹⁹
B ₁₂ -2'OMe	50% reduction of RFP fluorescence: 1.0 µM	N.A.	<i>E. coli</i> ; <i>S. enterica</i>	Giedyk et al. ⁸⁶
(KFF) ₃ K-LNA	MIC: 1.56–12.5 µM	Mouse peritonitis: 3 mg/kg	MRSA	Meng et al. ³⁸
(KFF) ₃ K-LNA/ps	Quorum sensing inhibition: 3.125–12.5 µM	Mouse skin infection: 40 µM	MRSA	Da et al. ¹²¹
(RXR) ₂ XB-aminoBNA ^{NC}	Resistance gene inhibition: 0.5 µM	<i>G. mellonella</i> model: 0.5 µM	<i>A. baumannii</i>	Lopez et al. ⁹⁴
pVEC-2'OMe-PS/DNA-2'OMe gapmer	MIC ₈₀ : 0.7 µM	N.A.	<i>L. monocytogenes</i>	Traykovska et al. ¹²²
pVEC-2'OMe-PS/DNA-2'OMe gapmer	MIC ₈₀ : 0.7 µM	N.A.	<i>L. monocytogenes</i> ; <i>S. aureus</i>	Traykovska and Penchovsky ¹²³
2'OMe encapsulated in DPP decorated with PEG2000-DSPE	Growth inhibition: 1 µM	Sepsis mice model: 1.5 mg/kg (225 nmol/kg ASOs)	ESBLs- <i>E. coli</i>	Chen et al. ¹²⁴
2'OMe/PGO	Growth inhibition (54%): 20 µM	N.A.	<i>M. smegmatis</i>	Skvortsova et al. ⁵²
5' and 3' hairpin modified PS/DNA	Growth inhibition: 10 µM	N.A.	<i>M. tuberculosis</i>	Harth et al. ¹²⁵
DNA-ASO loaded GO/alginate hydrogel	Biofilm inhibition: 10% (w/v) single-stranded DNA in 50 µg/mL GO	Mouse skin wound model: 10% (w/v) single-stranded DNA in 50 µg/mL GO	<i>S. aureus</i>	Wu et al. ¹²⁶
MLGNP	Growth inhibition (71%): 10 nM MLGNP synthesized at an initial ASOs concentration of 100 µM	N.A.	MRSA	Beha et al. ¹²⁹
GOx&HRP/ZIF-8/DNA-ASO	MIC: 16 µg/mL	Mouse skin wound model: 200 µg/mL	MRSA	Zhang et al. ¹³⁰
10 µg/L isoniazid + PS modified DNAzyme	Growth inhibition (63%): 5 µM	N.A.	<i>M. tuberculosis</i>	Li et al. ¹⁴⁸
ZNO/ampicillin/DNA nanoflower	MIC: 100 µg/mL DNA nanoflowers	Rabbit keratitis: 32 µg/mL ampicillin, 4 µg/mL ZnO, 100 µg/mL DNA nanoflowers	MRSA	Ran et al. ¹⁵⁴

(Continued on next page)

Carrier + oligonucleotide	<i>In vitro</i> antimicrobial activity	<i>In vivo</i> antimicrobial activity	Bacteria	Reference
12-bis-THA nanoplexes loaded with TFD	N.A.	Hamsters bearing intestinal infection; 2 mg/kg	<i>C. difficile</i>	Marin-Menéndez et al. ²⁵
TFD-THA-TP-SLN	Growth inhibition: 0.02–0.07 µg/mL	N.A.	<i>E. coli</i> K12	González-Paredes et al. ¹³⁴
cNLC-TFD	Resistance gene inhibition: 0.125 µM	N.A.	MRSA	Hibbitts et al. ⁸⁷

CGD, chronic granulomatous disease; EPC, egg phosphatidylcholine; MDR, multidrug resistance; MIC₅₀, the minimum inhibitory concentration of PNA required to inhibit 50% of *L. monocytogenes* isolates; N.A., not available; TP, triphalmitin; N/P ratio, amine/phosphate ratio.

To enhance their biological activity, CPPs have been engineered through the selection of their amino acid composition. For instance, ASOs conjugated to arginine (R)-rich peptides such as (RFF)₃KXB, (RFR)₄XB, and (RX)₆B have shown lower MICs in *E. coli* compared to their counterparts containing the (KFF)₃K peptide.^{40,41} Furthermore, the (RFF)₃KXB-PMO conjugate was found to be almost 3-fold more potent against *S. typhimurium* than the (KFF)₃KXB-PMO.⁴⁰

Another widely used CPP is the (RXR)₄XB peptide (and its (RXR)₄ derivative), which has been considered the most effective carrier of PNA and PMO in several bacteria, including *E. coli*, *P. aeruginosa*, *L. monocytogenes*, *Acinetobacter lwoffii* and *A. baumannii*, and *Streptococcus pneumoniae*.^{24,41,84,95,102} This peptide outperforms other equally effective permeabilizers such as the (RFF)₃R, (RFR)₄XB, (RX)₆B, and TAT (amino acid sequence GRKKRRRQRRYK, where G is glycine, R is arginine, K is lysine, Q is glutamine, and Y is tyrosine) peptides. Exceptions were noted in *Streptococcus pyogenes*, *Burkholderia cepacia*, and *B. anthracis*, where TAT, (RFF)₃RXB, and (RFF)₃R yielded higher antimicrobial activity (MIC: 1.25–15.6 µM) compared to (RXR)₄XB conjugates (MIC: 40–80 µM).^{16,18,36} These findings indicate that the potency of CPPs to permeabilize bacteria is greatly influenced by the amino acid composition. In fact, this was also concluded by Mellbye and colleagues.⁴¹ They observed that arginine (R) is more effective than lysine (K) in permeabilizing bacteria, which explains why (RXR)₄XB, (RFR)₄XB, (RX)₆B, and (RFF)₃KXB are generally more effective than the (KFF)₃K peptide. These findings are not only important to elucidate the reasons behind the differences in the efficiency of CPPs but can also be used to improve the specificity of antisense drugs against pathogenic bacteria.

It is worth noting, however, that these peptides and their respective conjugates exhibit varying levels of toxicity. For instance, (KFF)₃K-PNA displays toxicity in A549 cells at concentrations exceeding 5 µM,¹⁰³ whereas 10 µM of (RFF)₃XB-PMO does not exhibit any toxic effect in Caco-2 cultures.⁴⁰ TAT, when tested on HeLa and CHO cells, shows negligible effects on proliferation at concentrations up to 50 µM.¹⁰⁴ In mice, (RX)₆B-PMO was found to be toxic at a dose of 15 mg/kg,⁴¹ whereas (RXR)₄XB-PMO has been demonstrated to be nontoxic up to 3.75 mg/kg when administered intranasally.¹⁰⁵ When intravenously injected in rats, 15 mg/kg of (RXR)₄XB-PMO did not produce detectable toxicity.⁹⁹ It is important to note that unconjugated ASOs did not exhibit toxicity. Nevertheless, it is imperative to perform a direct comparison of toxicity using the same models, because susceptibility to toxic effects can vary among different cell lines. In addition, the body weight of animal models should be taken into consideration when assessing toxicity.⁴¹

Another interesting feature is the ability of CPPs to permeate both mammalian and prokaryotic cells. This property has been exploited to test the efficacy of CPPs conjugated to PNAs in treating intracellular infections caused by *Brucella suis* or *L. monocytogenes* *in vitro*.^{33,95} However, the susceptibility of *L. monocytogenes* to the

antisense drug varied depending on the CPP used, with the highest susceptibility in the following order: (RXR)₄XB > (RFR)₄XB = TAT > (KFF)₃K.⁹⁵ The improved performance of the (RXR)₄XB conjugate can be attributed to a double effect, which includes the increased permeabilization achieved by the (RXR)₄XB peptide in bacteria and its ability to evade endosomolytic agents in mammalian cells.¹⁰⁶ The (RXR)₄XB conjugates also showed an improvement in the survival of *Caenorhabditis elegans* larvae infected with *L. monocytogenes* at doses ranging from 15 to 30 μM.^{83,95}

The activity of CPP-ASO conjugates may be hindered by proteolytic degradation, because the breakdown of CPP sequences may reduce their capacity to penetrate bacterial envelopes. As shown by Yavari et al.³⁹ shorter versions of the (KFF)₃K peptide were found to be less effective in carrying PNAs in *E. coli*. Similarly, Mellbye et al.⁴¹ reported that truncated (RFF)₃KXB and (RX)₆B peptides carrying PMOs were also less effective. As such, a recurring characteristic of several CPPs is the presence of the -XB- motif at their C-terminal end, which is vital for improving their resistance to proteolysis, both in serum and within cells.⁷¹ Another strategy aimed at enhancing the stability of CPPs involves the use of D-isomeric peptides. Yavari et al.³⁹ and Mellbye et al.⁴¹ assessed the effectiveness of the D-isomeric forms of (KFF)₃K-PNA and (RFF)₃XB-PMO, respectively, and found that they exhibited potent antimicrobial activity against *E. coli* with MICs that were only 2-fold higher compared to CPPs with L-configuration (with values of 2–4 and 5 μM, respectively). The D-isomeric CPPs are also stable in both serum and intracellular environments,¹⁰⁷ making them suitable for systemic administration and treatment of intracellular infections. Furthermore, researchers have also shown that branched cationic peptides exhibit enhanced stability against proteolytic degradation and can transport charge-neutral ASOs into bacteria. For instance, Iubatti et al.¹⁰⁸ conjugated PNAs to cationic peptide dendrons comprising three generations of diaminobutanoic acid with eight terminal guanidinobutanoic acid derivatives. The dendron-PNA conjugates exhibited stability in both mouse and human serum and were noncytotoxic for HepG2 cells up to a concentration of 90 μM. In *in vitro* experiments, the dendron-PNA displayed potent antimicrobial activity against *E. coli*, with an MIC of 0.5 μM. However, it was 16-fold less effective against *K. pneumoniae*, a difference that may be attributed to distinctions in envelope features. Following intravenous administration, the conjugates were well tolerated in mice, even at doses up to 20 mg/kg, effectively treating multidrug-resistant *E. coli* peritonitis. Notably, dendron-PNA conjugates predominantly accumulated in the kidneys and liver up to 24 h postinjection. Given this distribution pattern, it is prudent to assess nephro- and hepatotoxicity before considering further applications.

As an alternative to CPPs, vitamins and DNA tetrahedrons have emerged as potential options for delivering antisense PNA to bacteria (Figure 1). For instance, vitamin B₁₂-PNA conjugates were used at a concentration of 5 μM and were able to inhibit the growth of *E. coli in vitro*. However, the effectiveness of these conjugates in the human body may not be as high as expected due to the saturation of B₁₂ re-

ceptors in the bacterial envelopes with free vitamin.²⁶ DNA tetrahedrons are potentially nontoxic and elicit low immunogenic responses, making them excellent candidates for drug delivery.^{109–111} They have been loaded with PNA targeting antibiotic-resistance genes, such as *bla*_{CTX-M-group 1} (encoding the β-lactamase CTX-M-group 1). The presence of 40 μM of these ASOs reduced the cefotaxime MIC from 35 to 16 mg/L,¹¹² consisting of a 2-fold increase in the cefotaxime antimicrobial activity. In addition, a similar DNA tetrahedron loaded with 0.75 μM of antisense PNA was found to effectively inhibit 50% of MRSA growth.³⁷ Despite the promising results, there are still doubts about the stability and mechanism of intracellular delivery. Studies have indicated that DNA tetrahedrons are susceptible to DNase digestion, necessitating protection against nuclease activity when administered systemically.^{113,114} Conversely, DNA tetrahedrons incubated for 12 h in 10% fetal bovine serum (FBS), human umbilical vein endothelial cells cell lysate, and *E. coli* lysate exhibited remarkable stability, as evidenced by nearly unchanged bands in an electrophoretic gel.¹¹⁵ Similar findings were reported by Li et al., who observed the stability of these structured DNA nanoparticles for 4 h in FBS and within cells.¹⁰⁹

As mentioned previously, the mechanism of intracellular DNA tetrahedron delivery in bacteria remains poorly understood. In a study using atomic force microscopy and scanning electron microscopy, it was observed that DNA tetrahedrons induce deformations in the membrane of *E. coli*, leading to cell shrinkage and the formation of pores, ultimately resulting in cytoplasmic leakage.¹¹⁵ The signal from fluorescently labeled DNA tetrahedrons also increases within the cytosol, indicating their ability to traverse bacterial envelopes.^{27,37,113,115} In contrast, labeled single-stranded DNA controls remained nearly undetectable, underscoring the necessity of the pyramid shape for permeabilizing both Gram-negative and Gram-positive envelopes. A common limitation of these studies was the labeling of a single strand of the DNA tetrahedron scaffold, which hinders drawing conclusions regarding the integrity of the nanoparticle. Consequently, labeling two different strands with a fluorescence resonance energy transfer pair could enable the assessment of DNA tetrahedron scaffold dissociation.^{109,113} This same strategy could also prove useful in determining whether a double-labeled single strand within the DNA tetrahedron scaffold remains intact or becomes cleaved following intracellular delivery.

A notable limitation of the previously discussed delivery strategies is their lack of selectivity, leading to interactions with mammalian cells and subsequently increasing the potential for toxicity. Addressing this issue, Liu et al.¹¹⁶ devised an innovative strategy for selectively delivering PNAs to drug-resistant bacteria. This approach involves antisense PNAs conjugated to glucose polymer-modified fluorescent silicon nanoparticles (GP-SiNPs-asPNA). The GP-SiNPs-asPNA (≈ 5.6 nm) exhibit an impressive capability to traverse bacterial envelopes through the bacteria-specific ATP-binding cassette (ABC) sugar transporter pathway, which is absent in mammalian cell membranes. These constructs effectively inhibited essential target genes in multidrug-resistant *E. coli* and MRSA at a low dose (MIC: 0.8 μM),

demonstrating minimal internalization by various human cell lines, including normal colon epithelial cells (NCM-460), colorectal cancer cells (CT26 cells), thyroid follicular carcinoma cells (FCT133), mouse urothelial epithelial cells, and human retinal pigment epithelial cells (ARPE-19). Collectively, these results demonstrate selectivity toward bacteria over mammalian cells. The GP-SiNPs-asPNA were also found to be noncytotoxic to ocular cells up to 60 μM , and they remained stable in 10% (v/v) FBS for 7 days. To assess the potential therapeutic effect of GP-SiNPs-asPNA, bacterial keratitis and endophthalmitis models were established in mice. The corneas of mice were treated with a 20- μL solution of GP-SiNPs-asPNA containing 1 μM of antisense PNA, resulting in bacteriostatic rates ranging from 98.6% to 99% after 5 days of treatment. Negligible topical and systemic toxicities were observed.

INTRACELLULAR DELIVERY OF ANIONIC ASOs

Anionic ASOs have shown potential as antimicrobials, with MICs ranging from 0.2 to 12.5 μM (Table 2). Unlike PNA and PMO, the delivery strategies for anionic oligonucleotides are more diverse, including lipid particles, peptides, vitamins, and DNA nanostructures (Figure 1). In addition, various (natural and synthetic) anionic nucleotides can be combined to create a limitless variety of chimeric structures that can either be highly resistant to nuclease degradation or capable of activating RNase H-mediated cleavage.^{15,27,38,42,49,50,85,94,117,118} One of the pioneering studies on the potential of anionic ASOs to suppress gene expression in bacteria used PS/DNA oligonucleotides encapsulated in liposomes formed by dipalmitoylphosphatidylcholine (DPPC) and dimyristoylphosphatidylglycerol (DMPG) to inhibit β -galactosidase activity in *E. coli* at 10–25 μM ASO concentration.¹¹⁷ Nevertheless, the loading of anionic oligonucleotides in anionic vesicles is not effective, but strategies have been developed to enhance its efficacy. One approach is to complex PS-ASOs with polyethylenimine (PEI) and then load the resulting polyplexes into anionic liposomes. Perche and colleagues⁴² successfully demonstrated this strategy, using it to inhibit the growth of *P. aeruginosa* and *E. coli*, by targeting the *acpP* mRNA with 1 μM PS-ASOs. At ASO concentrations ranging from 1 to 4 μM , the loaded liposomes showed no toxicity toward dendritic cells. Cytotoxicity only became apparent at ASO concentrations exceeding 8 μM , likely attributable to the cationic properties of PEI. Another similar construct with a different lipid formulation was used to target antibiotic resistance mechanisms. In this study, PS-ASOs, at doses from 0.5 to 18 μM , were able to restore the antimicrobial activity of antibiotics against MRSA, multidrug-resistant *P. aeruginosa*, and fluoroquinolone-resistant *E. coli*.^{15,49,50} Furthermore, the administration of 5–10 mg/kg of liposomal PS-ASOs in combination with a therapeutic dose of oxacillin significantly improved the survival of mice bearing MRSA septicemia.¹⁵ Unlike PNA and PMO, which often target regulatory sequences to block mRNA translation, these PS-ASOs were designed to target interior regions of the mRNA, forming heteroduplexes that can recruit RNase H activity.

As an alternative to liposomes, lipids moieties were also conjugated to PS/DNA oligonucleotides to form micellar structures that were able

to cross the envelope of an extended spectrum β -lactamases (ESBLs)-*E. coli* strain, thus restoring the antimicrobial activity of ceftriaxone.¹¹⁸ However, a thorough analysis of the antisense mechanism using qRT-PCR and western blotting failed to reveal any significant decrease in the expression of the *bla*_{CTX-M-15} gene. The authors suggested that the reduction in the ceftriaxone MIC may be a result of a specific effect on another gene or an off-target mechanism.

With the aim of improving the stability of ASOs, gapmers composed of PS/DNA and 2'OMe have been also tested. In this study, cationic bolaamphiphile nanoplexes loaded with 2'OMe-PS/DNA-2'OMe gapmers were designed to target and inhibit the growth of *Clostridium difficile*.⁸⁵ The nanoplexes displayed potent antimicrobial activity at doses as low as 0.2–0.8 μM . However, the authors noted that the cationic nature of the nanoparticles may cause antimicrobial activity at high concentrations, potentially reducing the specificity of the antisense drug. Furthermore, the cationic bolaamphiphile alone exhibits modest toxicity (half-maximal inhibitory concentration [IC₅₀] of 61 \pm 1 μM) in Caco-2 cells.²⁵ Despite this limitation, they demonstrated that 2'OMe-PS/DNA-2'OMe gapmers, once delivered, have potential as antisense antimicrobials.

In another study, DNA tetrahedrons, which have also been proven to be effective carriers of PNA in both *E. coli* and MRSA,^{37,112} were also used to deliver 2'OMe/PS/DNA mixmers. These mixmers were designed to prevent biofilm formation by *Streptococcus mutans*, and an MIC for these DNA tetrahedrons-mixmers of 0.75 μM was obtained.²⁷ An alternative DNA nanostructure was developed for delivering PS/DNA-ASOs into *S. aureus*. This structure comprises a DNA six-helix bundle (6HB) loaded with three ASOs.¹¹⁹ The 6HB/ASOs (0.2 μM 6HB containing 0.6 μM ASOs) were incubated with *S. aureus*, resulting in the inhibition of 53.2% of *ftsZ* gene expression. Consequently, the bacterial growth decreased to 57.6% after a 24-h incubation period. As anticipated for a construct assembled solely with DNA and PS/DNA, 6HB/ASOs exhibited virtually no cytotoxicity against human normal liver L02 cells at the antimicrobial concentration. In contrast to the DNA tetrahedron, 6HB did not penetrate *E. coli* cells, suggesting a selective behavior that favored the delivery in Gram-positive bacteria. The authors speculated that the 14-nm 6HB could traverse the recently imaged 60-nm pores in the *S. aureus* wall.¹²⁰

Taking a different approach, Giedyk et al.⁸⁶ used vitamin B₁₂ to deliver full 2'OMe ASOs in *E. coli* and *S. typhimurium* with the aim of inhibiting the gene that encodes for the red fluorescence protein (RFP). Nonetheless, it was found that B₁₂ may have limitations in delivering LNA-DNA-LNA gapmers and LNA/2'OMe mixmers in *E. coli*.⁷³

LNA has been shown to increase the stability of heteroduplexes, thereby enhancing the gene downregulation effect.⁵⁹ Thus, nanocarriers capable of delivering LNA (and its analog BNA) are highly sought after, but only CPPs have been successful in this regard. In three distinct works, LNA and aminoBNA^{NC} oligonucleotides were

conjugated with CPPs to target essential, virulence, and antibiotic-resistance genes, respectively, in drug-resistant bacteria. In the first case, LNA-ASOs were conjugated to the (KFF)₃K peptides, which effectively inhibited the growth of MRSA, with doses ranging from 1.56 to 12.5 μ M. Moreover, treatment with 3 mg/kg of the (KFF)₃K-LNA conjugate was effective in curing mice infected with MRSA.³⁸ The same research group used an 18-mer LNA/PS mixmer coupled with (KFF)₃K peptides to target the *agrA* (accessory gene regulator) mRNA, a component of the quorum sensing system in MRSA responsible for regulating the expression of virulence genes, including numerous toxins and degradative exoenzymes. Administering a dose of 40 μ M effectively prevented the development of necrosis and ulceration on the skin of mice afflicted with a skin infection. Moreover, it resulted in a reduction of more than 4 logs in the colony-forming units at the infection site.¹²¹ In another study, treatment with (RXR)₄XB-aminoBNA^{NC} (0.5 μ M), which targets the mRNA of the antibiotic-resistance *aac(6')-Ib* gene, restored the activity of amikacin.⁹⁴ In *Galleria mellonella* infected with *A. baumannii*, a mixture of 0.5 μ M (RXR)₄XB-aminoBNA^{NC} and 10 mg/kg amikacin was therapeutically effective. Despite these promising results, there are still limited studies demonstrating the ability of CPPs and anionic ASOs to form stable and effective conjugates in living organisms.

Recently, 2'OMe-PS/DNA-2'OMe gapmers were successfully delivered to *S. aureus* and *L. monocytogenes* by conjugating them with the CPP pVEC (amino acid sequence LLILRRRIRKQAHASHK, where L is leucine, I is isoleucine, R is arginine, K is lysine, Q is glutamine, A is alanine, H is histidine, and S is serine), inhibiting 80% of bacterial growth (MIC80) at 0.7 μ M (4.5 μ g/mL) of pVEC-ASO.^{122,123} The conjugates showed good biocompatibility up to 1 μ M tested in A549 human cells. Interestingly, the pVEC-ASO were designed to target two distinct riboswitches (TPP and S-adenosyl methionine I [SAM-I]) located in the 5' UTR of mRNAs in Gram-positive bacteria. This strategy enhances the selectivity for this bacterial group, as evidenced by their inability to influence the *E. coli* growth.

An alternative to linear cationic peptides involves the encapsulation of anionic ASOs within dendritic polypeptides (DPPs) decorated with PEG2000-DSPE (distearoylphosphatidylethanolamine).¹²⁴ The amphipathic DPP (amino acid sequence (acetyl-LWLLW)₂KKK(RRHR)₂, where L is leucine, W is tryptophan, K is lysine, R is arginine, and H is histidine) comprises two hydrophobic branches and two hydrophilic branches, interconnected by three lysine residues. This structure was used for the encapsulation of 2'OMe-ASOs demonstrating excellent biosafety with normal human small intestine epithelial cells and negligible hemolytic activity at 1 μ M. The DPP/ASO/DSPE-PEG construct demonstrated strong antibacterial effects *in vivo*, elevating the survival rate of septic mice infected with drug-resistant *E. coli* to 90% at a dose of 1.5 mg/kg (225 nmol/kg ASOs). Consistent with the *in vitro* findings, the mismatch control resulted in a 20% survival rate, indicating that the constructs lack specificity at the most effective tested concentration. The concentration-dependent specificity observed in DPP/ASO constructs aligns with findings reported in studies using linear CPP-ASO

conjugates.¹⁰² Furthermore, DPP/ASO/PEG2000-DSPE exhibited rapid accumulation in the kidneys and liver, similar to the pharmacokinetics observed in the dendron-PNA designed by Iubatti and collaborators.¹⁰⁸

In addition to being larger in size compared to traditional antibiotics, the negative charge of ASOs presents a barrier to their penetration into bacteria.⁹¹ To overcome such a limitation, Skvortsova et al.⁵² designed novel ASOs called phosphoryl guanidine oligo-2'-O-methylribonucleotide (2'OMe/PGO [phosphoryl guanidine oligo-2'-O-methylribonucleotide]) (Figure 1). The main advantage of the 2'OMe/PGO is the neutral internucleoside linkage, which is achieved by replacing the PO with a phosphoryl guanidine group. In addition to being nuclease resistant and having comparable affinity to 2'OMe oligonucleotides, the neutral charge of the 2'OMe/PGO ASOs made it possible for them to penetrate both macrophages and intracellular *Mycobacterium smegmatis*, even without the use of nanocarriers. The use of 20 μ M of ASOs (targeting the mRNA position [−10; 13]) to suppress the *ald* gene (which encodes alanine dehydrogenase) resulted in a 54% reduction in bacterial growth. Interestingly, Harth et al.¹²⁵ also developed ASOs that were able to penetrate mammalian cells without the use of nanocarriers and partially inhibit the *M. tuberculosis* infection. These ASOs were PS/DNA oligonucleotides (10 μ M) with 5' and 3' hairpin extensions. These modifications at the ends enhanced the internalization of the ASOs, leading to a reduction in bacterial growth by \sim 1.75 log units in broth culture medium and 0.4 log units in infected human THP-1 macrophages. Nonetheless, the effectiveness of 2'OMe/PGO and hairpin ASOs is likely limited to mycobacterial species because the unique features of their envelopes may allow for the penetration of these specific uncharged nucleic acids and structured oligonucleotides. Another factor contributing to the success of these ASOs could be the experimental conditions that may have facilitated the penetration of these oligonucleotides into the bacterial envelopes. As a result, it is unlikely that 2'OMe/PGO and hairpin ASOs will be effective in penetrating the envelopes of Gram-negative and Gram-positive bacteria without the assistance of nanocarriers.

Another approach evaluated ASO-loaded graphene oxide (GO)/alginate hydrogel for inhibiting *S. aureus* infection in a mouse skin wound model.¹²⁶ A dose of 10% (w/v) single-stranded DNA in 50 μ g/mL GO (2 μ L) was coadministered with a suspension of *S. aureus*. The hydrogel effectively impeded the progression of infection, as confirmed by histological examination 10 days postinjection. Although this approach holds promise for treating soft wound infections, addressing an established antimicrobial-resistant infection may necessitate higher doses of ASO-loaded GO, which could pose a significant toxicity risk.^{127,128} In addition, stability tests are imperative to confirm whether unmodified DNA-ASOs will maintain their integrity *in vivo*.

Distinct from previous approaches, Beha et al.¹²⁹ used gold nanoparticles coated with alternating layers of high-molecular-weight (25 kDa) branched PEI and anionic ASOs for inhibiting the

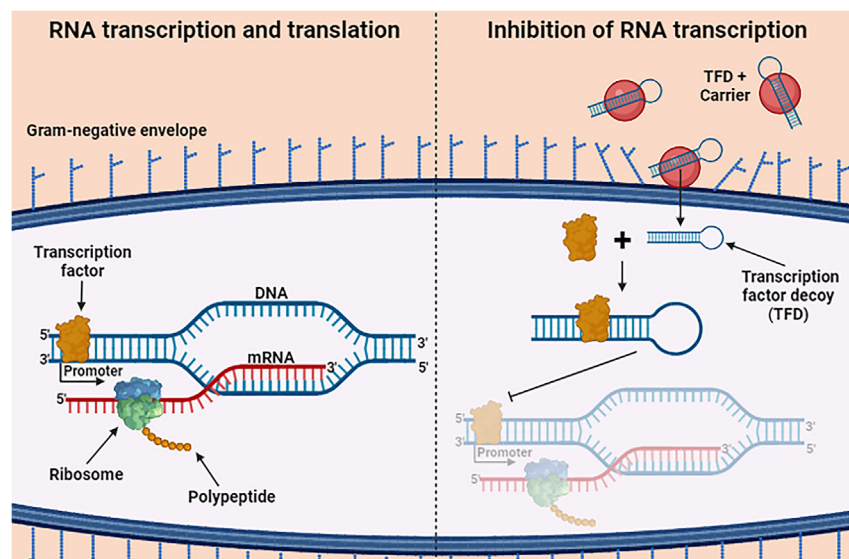


Figure 3. Inhibition of gene expression through the TFD mechanism

In absence of TFDs, the transcription factor binds to the promoter activating gene transcription. The mRNA is then translated by the ribosomes into a functional protein. The binding of the TFD to the transcription factor hinders the transcription initiation and downstream reactions, leading to the production of a protein. The gene expression is inhibited by arresting DNA transcription, rather than mRNA translation. (This figure was created with BioRender.com.).

codynamics of the constructs need thorough evaluation to confirm the safety of these antimicrobial agents.

TFD OLIGODEOXYNUCLEOTIDES

Oligonucleotides can be designed to sequester DNA binding proteins holding regulatory functions in the gene expression.¹³¹ This is the case

mecA gene in MRSA. The multilayer-coated gold nanoparticles (MLGNPs) demonstrated a 26% inhibition of *mecA* expression (with 10 nM MLGNP synthesized at an initial ASOs concentration of 100 μ M). The coadministration of MLGNP and oxacillin resulted in a 71% reduction in MRSA growth, whereas mismatch ASOs did not exhibit any inhibitory effects. However, ASOs only marginally contributed to increased potency, because PEI-coated gold nanoparticles alone reduced growth by 63%. This suggests that the PEI-coated gold nanoparticles permeated the MRSA envelope, facilitating the unhindered movement of oxacillin into the cytosol. Indeed, *mecA* expression was significantly influenced by cationic gold nanoparticles lacking ASOs. A positive aspect in favor of gold nanoparticles was the observed selectivity in penetrating bacteria rather than cocultured cells, with low cytotoxicity (85% viable cells after 24 h of incubation).

Although several studies have demonstrated the potential use of ASOs as adjuvants for antibiotics against drug-resistant bacteria,^{15,46–51,94,112,129} ongoing research is exploring novel synergies involving antimicrobial ASOs, metal ions, and systems that generate reactive oxygen species (ROS). Zhang et al.¹³⁰ constructed antimicrobial nanoparticles by encapsulating ROS-generating cascade enzymes (glucose oxidase [GOx] and horseradish peroxidase, HRP) within zeolite imidazole framework-8 (ZIF-8), followed by coating with DNA-ASOs (GOx&HRP/ZIF-8/ASO) through electrostatic interactions. Cytotoxicity testing on HeLa, MCF-7, and L02 cells revealed that GOx&HRP/ZIF-8/ASO nanoparticles are biocompatible at concentrations up to 80 μ g/mL, with negligible hemolytic activity observed at 512 μ g/mL. In mice with MRSA skin infection, subcutaneous administration of 200 μ g/mL GOx&HRP/ZIF-8/ASO with glucose cleared the infection after 14 days of treatment. In addition, examination of the major organs, liver and kidney function tests, and blood tests of the mice confirmed the *in vivo* biocompatibility of the constructs. Nevertheless, the pharmacokinetics and pharma-

for TFDs, which represent a novel class of nucleic acid-based drugs (Figure 1).¹² TFDs are short double-stranded DNA molecules that contain the DNA binding site of a transcription factor that targets a specific *cis*-regulatory promoter sequence of the target gene (Figure 3). Therefore, TFDs recruit the binding of a specific transcription factor, which would usually bind to the promoter of a gene to initiate the transcription. In this way, the inhibition of the gene expression is performed by arrest of the DNA transcription rather than the mRNA translation.

The successful demonstration of gene regulation in bacteria through TFDs has been achieved. Wang et al.¹³² designed TFD oligonucleotides that effectively activated eight silent gene clusters in various *Streptomyces* strains. In another study, TFDs were engineered to suppress the arginine production pathway repressor in *E. coli*, resulting in a 16-fold increase in arginine production.¹³³ Furthermore, TFDs directed toward various gene regulators known to influence *E. coli* survival under exposure to pinene (a monoterpene toxic to *E. coli* at 0.5%, v/v) notably improved bacterial resilience against pinene-induced stress.¹³³ This enhancement was observed in a concentration-dependent manner for TFDs.

STRATEGIES TO ENHANCE TFD RESISTANCE AGAINST NUCLEASES

Nuclease sensitivity is a prevalent challenge faced by nucleic acid-based technologies developed for *in vivo* applications. Indeed, during circulation in the human body and following intracellular delivery, exogenous nucleic acids are vulnerable to nuclease degradation. To enhance resistance against nuclease activity, antimicrobial TFDs have been designed with a hairpin shape (Figure 1),^{25,87,134} in contrast to the conventional structure that exposes nucleotide residues at both terminal ends.^{12,135} The hairpin TFD structure enhances resistance to exonucleases by shielding terminal nucleotide residues at one end.¹² However, TFDs remain susceptible to endonuclease degradation.

To enhance resistance, PS internucleoside linkages can be introduced into the backbone of TFD.^{136,137}

Alternative designs aimed to incorporate PNA into TFDs, but initial efforts using PNA duplexes and PNA/DNA heteroduplexes failed to recognize transcription factors. PNA duplexes and PNA/DNA heteroduplexes adopt structural conformations that do not mimic DNA duplexes. In this scenario, this structural difference impedes their binding to the target transcription factor.^{138,139}

A closely analogous DNA duplex structure was developed by Romaneli et al.¹³⁸ They engineered a PNA-DNA-PNA duplex resembling the gapper structure found in ASOs (Figure 1). In this configuration, a 13-mer DNA duplex containing the transcription factor binding site is flanked by three paired PNA segments. The PNA-DNA-PNA chimera, designed to mimic the nuclear factor κ B site found within the long terminal repeat (LTR) of the HIV-1 virus, successfully inhibited the interactions between HIV-1 LTR and the proteins p50, p52, and nuclear factors from B-lymphoid cells. The same research group also demonstrated the effectiveness of the PNA-DNA-PNA chimera as a decoy for the Sp1 family, a group of transcription factors implicated in the regulation of the expression of several genes relevant to human pathologies.¹³⁹ However, achieving stability against nucleases was only partially successful, because the PNA-DNA-PNA chimera remained susceptible to endonucleases.¹³⁸ This issue could be addressed by synthesizing the DNA duplex with PS internucleoside linkages.^{136,137}

Alternatively, enhanced stability against both exo- and endonucleases can be attained by integrating two adjacent LNA substitutions at the double-stranded terminal ends of the TFDs (Figure 1), while preserving their binding affinity for the target protein.¹³⁵ On the contrary, when paired LNAs are placed within the double strand containing the binding motif, TFDs exhibit a decreased binding affinity for the target. Even a single LNA substitution in a position that affects the conformation of the protein binding sequence significantly diminishes the affinity for the transcription factor.^{135,140} Nonetheless, LNAs can be strategically incorporated into one strand of the protein-binding sequence of TFDs to enhance nuclease stability. It is crucial to meticulously select the position to ensure the retention of affinity for the target. When comparing PNA-based TFDs to LNA-based TFDs, the latter design is likely to be more advantageous due to the greater solubility of LNAs and their simpler synthesis using standard techniques.^{135,138–140}

INTRACELLULAR DELIVERY OF TFDs IN BACTERIA

The antimicrobial activity of TFDs was first demonstrated by Marin-Menendez et al.²⁵ They used nanoplexes assembled by complexation of hairpin TFDs (54-mer) and the cationic 12,12'-(dodecane-1,12-diyl)bis(9-amino-1,2,3,4-tetrahydroacridinium) bolaamphiphile (12-bis-THA) (Figure 1), to then target the SigH transcription factor in *C. difficile*. In hamsters bearing intestinal *C. difficile* infection, a dose of 2 mg/kg of TFDs rescued the animals from the lethal infection, whereas the scrambled oligonucleotide had no effect. However,

cationic bolaamphiphiles are potentially toxic to bacteria,⁸⁵ which may affect the selectivity of the antimicrobial drugs and interfere with the commensal population in the bowel. In addition, these nanoplexes exhibited mild cytotoxicity in Caco-2 cells, with an IC₅₀ of 68 ± 2 μM.

In another work, the antimicrobial activity of a 59-mer hairpin TFD targeting the ferric uptake regulator (FUR) transcription factor was tested.¹³⁴ In this case, cationic bolaamphiphile was replaced by solid lipid nanoparticles (SLNs) (Figure 1) that inhibited the *E. coli* growth (*in vitro*) at TFD concentrations ranging from 0.02–0.07 μg/mL, depending on the SLN formulation. The scrambled TFD lacking the FUR transcription factor binding site had no antimicrobial activity confirming the specificity of the FUR TFD. SLN also provides protection to TFD against nucleases, which is beneficial for improving the bioavailability of the cargos.¹³⁴

Moreover, Hibbitts et al.⁸⁷ demonstrated the therapeutic potential of a 40-mer TFD targeting the WalR two-component transcription regulator in *S. aureus*, a transcription factor controlling cell wall metabolism, membrane composition, and resistance to vancomycin.^{141,142} The TFD structure mimics the typical WalR binding sites within the *S. aureus* *lytM* promoter consisting of two TGTAAT hexamers separated by five nucleotides.⁸⁷ The presence of two repeated hexamers is necessary for the recognition of the promoter and the binding of the WalR transcription factor. In the absence of antibiotics, the WalR TFD loaded on a cationic nanostructured lipid carrier (cNLC) did not show significant antimicrobial activity against MRSA; however, when TFD-loaded nanoparticles (0.125 μM TFD) were coadministered with a sub-MIC concentration of vancomycin (0.6 μg/mL), the bacterial growth was reduced to 46% in relation to the untreated control. The TFD-cNLC was also biocompatible because it was noncytotoxic at the concentration used to inhibit the bacteria growth, and the hemolytic activity was below 10%.

Although these findings illustrate the potential of TFDs as novel therapeutic drugs against antibiotic-resistant bacteria, it is essential to conduct proper experiments to verify the interaction between the TFDs and the theoretical target, thereby validating the inhibitory mechanism. For instance, Hibbitts et al.⁸⁷ used a TFD designed to target the WhiB7 transcription factor binding site in *Mycobacteria* as a control to demonstrate the specificity of the WalR TFD. However, the WhiB7 TFD is shorter (30-mer) when compared to the WalR TFD. Using a scrambled TFD would provide considerably more reliable results.

DNAzymes

DNAzymes are catalytic DNA molecules that can act as specific RNA endonucleases once they bind to the target RNA (Figure 4).⁵⁸ Compared to ribozymes (catalytic RNA molecules), DNAzymes have several advantages: they are easier to synthesize, less sensitive to chemical and enzymatic degradation, more specific (which prevents *in vivo* side effects), and nonimmunogenic.^{143,144} The 10–23 DNAzyme has been studied as a potential antimicrobial drug (Figure 1),^{144–148} and it consists of a 15-deoxyribonucleotide catalytic

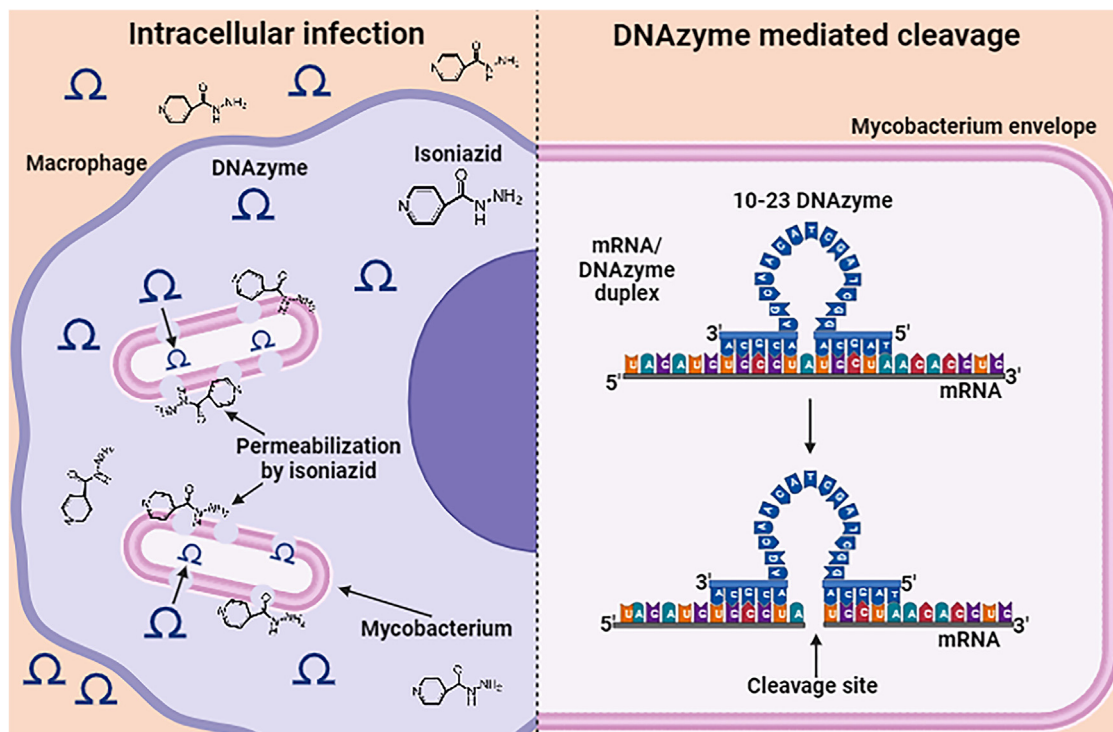


Figure 4. Inhibition of the mRNA translation through the DNAzyme cleavage mechanism

The DNAzyme arms bind to the target mRNA, and the catalytic core cleaves the PO linkage between adenine and uracil (AU) nucleosides hindering mRNA translation. Afterward, the DNAzyme releases the cleaved mRNA molecule. (This figure was created with [BioRender.com](#)).

core (5'-GGCTAGCTACAACGA-3') with two arms for substrate recognition (7- to 12-mer each). This DNAzyme can cleave a specific PO linkage between an unpaired purine (A, G) and a paired pyrimidine (C, U) under physiological conditions.¹⁴³

Chen et al.¹⁴⁵ investigated the catalytic efficiency of two 10–23 DNAzymes (35-mer each), one (Dz_1) targeting the start codon region ([–6; 19] position) and the other (Dz_2) binding to a downstream position ([469; 494]) of the β -lactamase mRNA in an β -lactam-resistant *E. coli*. Both DNAzymes reduced the β -lactamase activity, but the start codon region was the least efficient inhibitory position ($Dz_1 = 27.2\%–39.1\%$ and $Dz_2 = 39.6\%–44\%$). The results showed that the efficiency of DNAzymes in inhibiting gene expression and lowering β -lactamase activity was dependent on the position of the target sequence. This behavior is comparable to that observed with ASOs. Aiming to increase the catalytic activity, the two DNAzymes were fused to form a di-DNAzyme (Figure 1) consisting of two catalytic cores. This di-DNAzyme showed a higher inhibitory effect (57.7%–62.6%) than the two mono-DNAzymes. The increased catalytic efficiency was due to the enhanced interaction between the di-enzyme and the substrate, which resulted from the availability of two target positions for binding. However, the long length (70-mer) of the di-DNAzyme may prevent its internalization in bacteria. In fact, the DNAzymes were delivered *in vitro* using electroporation, a method that may be challenging to apply *in vivo*.

STRATEGIES TO ENHANCE DNAZYME RESISTANCE AGAINST NUCLEASES

Even though DNAzymes are more resistant to degradation than ribozymes, DNAzymes are still susceptible to nuclease degradation, like any DNA molecule. To increase their stability, Hou et al.^{144,146} designed two DNAzymes (34-mer each) with PS-modified arms that target the mRNA of the β -lactam resistance genes *blaR1* and *mecR1* in *S. aureus*. Each DNAzyme partially restored the antimicrobial activity of oxacillin in a concentration-dependent manner (5–15 $\mu\text{g}/\text{mL}$). Transcriptomic analysis confirmed the reduction of the target RNA, demonstrating the specificity of the DNAzyme.¹⁴⁶ However, complete eradication of the β -lactam resistance was only achieved by double targeting the *blaR1* and *mecR1* mRNAs, with both DNAzymes at 10 mg/L each.¹⁴⁷ Co-inhibition of *blaR1* and *mecR1* decreased the MIC of oxacillin from 1,024 to 1 mg/L, whereas individually, the susceptibility of MRSA to the antibiotic was only partially restored (512 and 256 mg/L, respectively).

Despite having improved stability, PS-oligonucleotides are still highly sensitive to nucleases and have lower binding affinities to RNA than nonmodified DNA.^{59,149} In contrast, 2'OMe and LNA incorporated in the substrate recognition arms can increase the binding affinity and nuclease resistance (Figure 1).^{149,150} Interestingly, the inclusion of 2'OMe in the catalytic core of DNAzymes can also improve the stability against nucleases, without compromising the folding of the

catalytic loop. Nonetheless, it also leads to a 50% decrease in its activity in a cell-free system. Modification of the recognition arms with LNA (also known as LNAzyme) accelerates the reaction kinetics of DNAzymes in single turnover experiments due to the enhanced binding affinity to the target RNA.¹⁴⁹ In multiple turnover conditions, however, the catalytic activity is reduced, presumably, due to a slower product release. To deal with this issue, α -L-LNA can replace the D-isomer, thus lowering the hybridization energy and, consequently, enhancing the product-DNAzyme dissociation.¹⁵¹ In cell line cultures, LNAzymes have shown an inconsistent performance, because their catalytic efficiency is greatly dependent on the cell type. This observation cannot be attributed to the improper selection of the binding site because ASOs targeting the same region in the mRNA effectively downregulate gene expression.¹⁵² Jakobsen et al.¹⁵³ also observed that LNA-modified ASOs are more potent inhibitors of gene expression than LNAzymes, but the catalytic oligonucleotides were still effective in suppressing HIV-1 production in HEK 293T cells. These findings indicate that LNAzymes are active in living cells; however, they may require a more exhaustive selection of the binding site in the tertiary structure to enhance the cleavage of the targeted mRNA.¹⁵¹

INTRACELLULAR DELIVERY OF DNAzymes IN BACTERIA

As briefly mentioned above, a common limitation of the studies involving bacteria and DNAzymes is the use of electroporation to internalize the catalytic oligonucleotides.^{144–147} To overcome such a limitation, Li et al.¹⁴⁸ combined a chemical membrane permeabilizer (isoniazid) with the DNAzymes to treat intracellular *M. tuberculosis* infection. A PS-modified DNAzyme was designed to downregulate the *icl* gene (coding the isocitrate lyase, a crucial enzyme for *M. tuberculosis* metabolism in the latent state). *In vitro*, *M. tuberculosis*-infected macrophages were treated with a subinhibitory concentration of isoniazid (10 μ g/L) to soften the bacteria envelope, allowing the internalization of DNAzymes (5 μ M) or the scrambled oligonucleotide. The *icl* protein expression only decreased with the DNAzyme treatment as well as 63% of the bacteria burden. Interestingly, the mixture of the DNAzymes and isoniazid had no effect on *M. tuberculosis* grown in culture medium, thereby showing that the *icl* gene is essential only for bacteria survival in infected macrophages.

Recently, Ran et al.¹⁵⁴ engineered a construct based on DNA nanoflower structures, prepared using the isothermal rolling circle amplification method.^{155,156} This construct involved the fusion of a DNAzyme targeting the *mecR1* (*mecA* gene regulator)¹⁵⁷ mRNA with an anti-*S. aureus* aptamer, resulting in the formation of a DNA nanoflower system.¹⁵⁴ The DNAzyme-aptamer nanoflower was further loaded with both zinc oxide (ZnO) nanoparticles and ampicillin (particle size of 95 nm). The aptamer played a crucial role in enhancing bacterial binding, whereas the ZnO nanoparticles functioned to disrupt biofilms, thereby facilitating the penetration of DNA nanoflowers and ampicillin into bacteria. The MIC of ampicillin against MRSA decreased from 128 to 32 μ g/mL, representing

a 4-fold reduction when loaded in ZnO/DNA nanoflowers. The optimized formulation, consisting of 32 μ g/mL ampicillin, 4 μ g/mL ZnO, and 100 μ g/mL DNA nanoflowers, effectively inhibited 98% of bacteria in biofilm form, underscoring its potent antimicrobial activity. It is noteworthy, however, that the control group, comprising ampicillin and ZnO nanoparticles, still contributed significantly, with 80% of the antimicrobial potency. Notably, the DNAzyme acted as an additional adjuvant to ampicillin in enhancing the antimicrobial activity. Using an eye drop delivery system, the ZnO/ampicillin/DNA nanoflower construct was administered to rabbits with MRSA keratitis. Remarkably, it proved effective in treating the infection within a 12-day period. Moreover, *in vitro* studies demonstrated negligible toxicity in human corneal epithelial cells, and local toxicity tests conducted on rabbit eyes revealed no adverse effects.¹⁵⁴

As discussed previously, the delivery of large oligonucleotides into bacteria continues to pose a significant obstacle to the development of effective oligonucleotide drugs. The ability of nanocarriers to internalize longer than 30-mer oligonucleotides in different bacteria was not extensively demonstrated despite some achievements *in vitro* using lipid vesicles and cationic bolaamphiphiles.^{25,42,87,134,158} Fortunately, LNAzymes have been investigated, holding shorter substrate recognition arms that allow shortening the overall oligonucleotide length.^{149,151}

CONCLUSIONS

Antimicrobial nucleic acids are an emerging class of drugs with the potential to combat AMR infections. Depending on their mechanism of action, these nucleic acids are designed with specific structures using a selection of nucleic acid analogs. However, some approaches are more promising than others, due to higher biological stability or simpler design. In this regard, ASOs are the most promising antimicrobial drugs because they offer good *in vivo* stability and have a relatively simple design. TFDs are potential alternatives to ASOs, although the process of identifying nucleic acid sequences that can bind to bacterial transcription factors with high affinity and specificity is complex and time-consuming. DNAzymes, in theory, can inhibit gene expression at a lower dose than ASOs since a single molecule can cleave many RNA targets in multiple turnover conditions. However, delivering functional DNAzymes into bacteria remains a challenging problem to solve.

Despite the fact that TFDs have also shown activity *in vivo*,²⁵ ASOs have been more frequently demonstrated to exhibit antimicrobial activity *in vitro* and in animal models.^{15,16,18,24,36,38,41,82,83,94,95} ASOs exhibit significant heterogeneity in design, including variation in length, sequence, and chemical structure. PNA and PMO analogs are generally the most effective at downregulating the expression of essential genes in both Gram-negative and Gram-positive bacteria. Charge-neutral oligomers have good stability against nucleases and can be designed to target regulatory sequences in mRNA and sterically block the assembly of the ribosomal apparatus. CPPs are used to deliver these antisense oligomers, and their effectiveness is

influenced by the ability of CPPs to deliver the oligomers to the cytosol. Therefore, the CPPs, in conjunction with the oligomer, modulate the selectivity of these antisense drugs.

Anionic oligonucleotides are often loaded in cationic lipid vectors. The positive charge of the lipid vectors has a dual function, facilitating efficient entrapment of the anionic ASOs and increasing the affinity of the constructs against both Gram-negative and Gram-positive bacteria.⁷² However, cationic lipid vectors are known to induce toxic events,^{159–161} necessitating the use of ASOs with high inhibitory potency to maintain the nanocarrier at biocompatible doses. Thus, it is crucial to select the most sensitive sequences in the mRNA to maximize the antisense inhibitory effect. In addition, recruiting the RNase H activity is desirable to increase the likelihood of effectively blocking the translation of the target mRNA. Due to their high efficiency in inhibiting RNA translation and improved biological stability, LNA-modified gapmers are potentially promising ASOs to combine with cationic lipid vectors. However, various delivery systems have been recently introduced as alternatives to cationic vectors. These include DNA nanostructures,^{27,119} Zn-based nanomaterials,^{130,154} gold nanoparticles,¹²⁹ GO/alginate hydrogel,¹²⁶ and a glucose polymer that mimics the Trojan horse antibiotic strategy.¹¹⁶ Despite the improved selectivity of these recent delivery strategies against bacteria rather than mammalian cells (which, in turn, can contribute to reducing toxicity), other components in the formulations exhibited significant and nonspecific antimicrobial activity. Therefore, comprehensive studies are required to better characterize these novel delivery strategies and properly evaluate their *in vivo* stability, pharmacokinetics, and pharmacodynamics.

TFDs are promising in inhibiting the expression of both essential and antibiotic-resistant genes at low oligonucleotide concentrations. This, in turn, allows for the administration of noncytotoxic doses of cationic vectors. However, the effectiveness of TFDs in controlling bacterial infections in animal models was poorly demonstrated, making it difficult to determine their overall effectiveness *in vivo*. Indeed, *in vitro* studies remain inconclusive concerning the inhibitory mechanism, primarily due to a lack of comprehensive research. This serves as an additional limitation that hinders the advancement of TFDs as effective antimicrobial agents.

DNAzymes can catalyze the cleavage of RNA on their own as demonstrated in cell-free experiments and in bacteria that have been permeabilized by electroporation.^{144–147} Despite their potential, DNAzymes face several challenges *in vivo* that may prevent them from achieving their goals. One such challenge is the long length of the oligonucleotide, which makes delivery to bacteria difficult. Another issue is the compatibility of DNAzymes with nucleic acid analogs. Depending on the type and position of insertion, these analogs can compromise the folding of the catalytic loop or slow down catalytic activity. Finally, selecting target sequences can be complex due to the limited availability of sterically unimpeded stretches in RNAs. Due to these constraints, DNAzymes are still far from *in vivo* applications.

It is unclear whether antimicrobial nucleic acids drugs will be effective against mutations that prevent the interaction of nanocarriers with bacteria or inactivate the functions of nucleic acids. If a mutation affects the ability of nanocarriers to bind or permeabilize bacteria, then redesigning the nucleic acids-nanocarrier constructs will be necessary. To anticipate this issue, it may be necessary to design nucleic acids drugs using different nanocarriers. In contrast, if a point mutation prevents antimicrobial nucleic acids from binding to the target, then the oligonucleotide sequence can be easily redesigned to restore inhibitory activity against the mutant bacteria. To assess the impact of mutations on the effectiveness of antimicrobial nucleic acids, studies that evaluate how these exogenous molecules and nanocarriers can trigger resilient mechanisms in bacteria will become crucial sooner rather than later.

There may be potential side effects associated with the administration of cationic vectors and the unspecific interactions of nucleic acids in the cytoplasm of human cells, which could cause toxicity. Specifically, cationic vectors have been shown to exhibit dose-dependent cytotoxicity and hemolytic activity, requiring proper dosage to control potential side effects.^{99,100,158} To improve selectivity and minimize off-target accumulation in tissues, the constructs can be modified by adding polymers and targeting ligands.^{71,162–164} Nucleic acids with excessive affinity may hybridize with off-target RNAs, interfering with the normal cell metabolism.^{60,61} To prevent nonspecific binding, the melting temperature of antimicrobial nucleic acids must be carefully adjusted and kept as low as possible. However, tests must be run to verify the specificity of the antimicrobial nucleic acids. This includes *in silico* analysis to screen for potential off-target interactions, and microarrays or qRT-PCR to evaluate the expression levels of off-target genes.¹⁶⁵ In addition, the translation levels of RNAs can be analyzed using western blotting.⁶¹

Despite the many developments in therapeutic nucleic acids for treating bacterial infections, this field is still in its infancy. The progress of antimicrobial nucleic acids in medicine is being hindered by the lack of comprehensive studies in animal models and humans demonstrating the effectiveness and biocompatibility of these treatments. Nonetheless, oligonucleotide drugs for treating chronic diseases are already available on the market, as well as nucleic acid-based vaccines to protect against infectious diseases such as severe acute respiratory syndrome-coronavirus-2. The success of these innovative medicines is expected to enhance confidence in nucleic acid-based drugs, which in turn may increase the attractiveness of the antimicrobial nucleic acids to new investors and researchers.

In the field of antimicrobial drugs, ASOs constructed from PNA or PMO and coupled with CPPs have proven to be the most promising nucleic acid-based candidates. They have undergone extensive validation in numerous *in vitro* models and, albeit less frequently, in animal models. Given that PMO has already received approval for the treatment of chronic diseases, PMO-CPP conjugates appear to be the most suitable candidates for achieving rapid progress in this field. Nevertheless, from our perspective, there is an opportunity to

enhance the versatility of this technology further by refining the design to facilitate precise adjustments of the characteristics of the constructs. Moreover, incorporating mechanisms for recruiting RNase H holds the potential to significantly augment the effectiveness of these antimicrobial drugs. In this context, LNA mixmers and LNA gapmers stand out as promising candidates in the pursuit of novel antimicrobial agents. It is important to highlight that linear CPP-ASO can also be enclosed within delivery systems that offer superior pharmacokinetic profiles compared to standalone CPP-ASO. Liposomes, for instance, with their extensive surface area, have the capacity to accommodate polymers and targeting ligands, thereby enabling the modulation of biodistribution, selectivity, and toxicity.

ACKNOWLEDGMENTS

This work was financially supported by: (1) LA/P/0045/2020 (ALICE), UIDB/00511/2020, and UIDP/00511/2020 (LEPABE), funded by national funds through FCT/MCTES (PIDDAC); (2) Projects POCI-01-0145-FEDER-016678 (Coded-FISH), POCI-01-0145-FEDER-030431 (CLASInVivo), and 2022.07654.PTDC (NAMSa), funded by FEDER funds through COMPETE2020–Programa Operacional Competitividade e Internacionalização (POCI), and by national funds (PIDDAC) through FCT/MCTES; (3) Project 2SMART - engineered Smart materials for Smart citizens, with reference no. NORTE-01-0145-FEDER-000054, supported by Norte Portugal Regional Operational Programme (NORTE 2020), under the PORTUGAL 2020 Partnership Agreement, through the European Regional Development Fund (ERDF); (4) project DELNAM - European Union's Horizon 2020 research and innovation program under grant agreement no. 810685; (5) Project EXPL/NAN-MAT/0209/2021 supported by Fundação para a Ciência e a Tecnologia; (6) FCT supported J.A.L. under the Scientific Employment Stimulus - Institutional Call - (CEE-CINST/00049/2018); and (7) Ph.D. fellowship developed under the doctoral program in Chemical and Biological Engineering (PDEQB) NORTE-08-5369-FSE-000028, co-financed by the Northern Regional Operational Program (NORTE 2020) through Portugal 2020 and the European Social Fund (ESF).

AUTHOR CONTRIBUTIONS

L.M. conceptualized and wrote the initial manuscript and created the figures. N.M.G., R.S.S., J.A.L., and M.C.P. conceptualized and revised the manuscript. N.F.A. conceptualized, supervised, and revised the manuscript.

DECLARATION OF INTERESTS

The authors declare no competing interests.

REFERENCES

- O'Neill, J. (2014). Antimicrobial Resistance: Tackling a crisis for the health and wealth of nations. *Rev. Antimicrob. Resist.* 1–16.
- Rather, I.A., Kim, B.C., Bajpai, V.K., and Park, Y.H. (2017). Self-medication and antibiotic resistance: Crisis, current challenges, and prevention. *Saudi J. Biol. Sci.* 24, 808–812.
- Rossolini, G.M., Arena, F., Pecile, P., and Pollini, S. (2014). Update on the antibiotic resistance crisis. *Curr. Opin. Pharmacol.* 18, 56–60.
- Ventola, C.L. (2015). The Antibiotic Resistance Crisis Part I: Causes and Threats. *P&T* 40, 277–283.
- Zhu, X., Radovic-Moreno, A.F., Wu, J., Langer, R., and Shi, J. (2014). Nanomedicine in the Management of Microbial Infection - Overview and Perspectives. *Nano Today* 9, 478–498.
- CDC (2019). CDC Antibiotic Resistance Threats in the United States, 2019 (U.S. Department of Health and Human Services).
- OECD & ECDC (2019). Antimicrobial Resistance. Tackling the burden in the European Union. In Briefing note for EU/EEA Countries (OECD).
- Stephens, L.J., Werrett, M.V., Sedgwick, A.C., Bull, S.D., and Andrews, P.C. (2020). Antimicrobial innovation: a current update and perspective on the antibiotic drug development pipeline. *Future Med. Chem.* 12, 2035–2065.
- Otterson, K., and Rex, J.H. (2020). Evaluating for-profit public benefit corporations as an additional structure for antibiotic development and commercialization. *Transl. Res.* 220, 182–190.
- McKenna, M. (2020). The antibiotic paradox: why companies can't afford to create life-saving drugs. *Nature* 584, 338–341.
- Bai, H., and Luo, X. (2012). Antisense Antibacterials: From Proof-Of-Concept to Therapeutic Perspectives. In *A Search for Antibacterial Agents*, V. Bobbarala, ed. (InTech), pp. 319–344.
- Hecker, M., and Wagner, A.H. (2017). Transcription factor decoy technology: A therapeutic update. *Biochem. Pharmacol.* 144, 29–34.
- Hu, J., Xia, Y., Xiong, Y., Li, X., and Su, X. (2011). Inhibition of biofilm formation by the antisense peptide nucleic acids targeted at the *motA* gene in *Pseudomonas aeruginosa* PAO1 strain. *World J. Microbiol. Biotechnol.* 27, 1981–1987.
- Mellbye, B.L., Weller, D.D., Hassinger, J.N., Reeves, M.D., Lovejoy, C.E., Iversen, P.L., and Geller, B.L. (2010). Cationic phosphorodiamidate morpholino oligomers efficiently prevent growth of *Escherichia coli* *in vitro* and *in vivo*. *J. Antimicrob. Chemother.* 65, 98–106.
- Meng, J., Wang, H., Hou, Z., Chen, T., Fu, J., Ma, X., He, G., Xue, X., Jia, M., and Luo, X. (2009). Novel anion liposome-encapsulated antisense oligonucleotide restores susceptibility of methicillin-resistant *Staphylococcus aureus* and rescues mice from lethal sepsis by targeting *mecA*. *Antimicrob. Agents Chemother.* 53, 2871–2878.
- Greenberg, D.E., Marshall-Batty, K.R., Brinster, L.R., Zarembek, K.A., Shaw, P.A., Mellbye, B.L., Iversen, P.L., Holland, S.M., and Geller, B.L. (2010). Antisense phosphorodiamidate morpholino oligomers targeted to an essential gene inhibit *Burkholderia cepacia* complex. *J. Infect. Dis.* 201, 1822–1830.
- Liang, S., He, Y., Xia, Y., Wang, H., Wang, L., Gao, R., and Zhang, M. (2015). Inhibiting the growth of methicillin-resistant *Staphylococcus aureus* *in vitro* with antisense peptide nucleic acid conjugates targeting the *ftsZ* gene. *Int. J. Infect. Dis.* 30, 1–6.
- Panchal, R.G., Geller, B.L., Mellbye, B., Lane, D., Iversen, P.L., and Bavari, S. (2012). Peptide conjugated phosphorodiamidate morpholino oligomers increase survival of mice challenged with Ames *Bacillus anthracis*. *Nucleic Acid Therapeut.* 22, 316–322.
- Jepsen, J.S., Sorensen, M.D., and Wengel, J. (2004). Locked Nucleic Acid: A Potent Nucleic Acid Analog in Therapeutics and Biotechnology. *Oligonucleotides* 14, 130–146.
- Nielsen, P.E. (2010). Peptide Nucleic Acids (PNA) in Chemical Biology and Drug Discovery. *Chem. Biodivers.* 7, 786–804.
- Summerton, J.E. (2006). Morpholinos and PNAs Compared. In *Peptide Nucleic Acids, Morpholinos and Related Antisense Biomolecules*, C.G. Janson and M.J. During, eds. (Springer), pp. 89–133.
- Moreira, L., Guimarães, N.M., Santos, R.S., Loureiro, J.A., Pereira, M.C., and Azevedo, N.F. (2023). Oligonucleotide probes for imaging and diagnosis of bacterial infections. *Crit. Rev. Biotechnol.*
- Bai, H., You, Y., Yan, H., Meng, J., Xue, X., Hou, Z., Zhou, Y., Ma, X., Sang, G., and Luo, X. (2012). Antisense inhibition of gene expression and growth in gram-negative bacteria by cell-penetrating peptide conjugates of peptide nucleic acids targeted to *rpoD* gene. *Biomaterials* 33, 659–667.

24. Geller, B.L., Marshall-Batty, K., Schnell, F.J., McKnight, M.M., Iversen, P.L., and Greenberg, D.E. (2013). Gene-silencing antisense oligomers inhibit acinetobacter growth *in vitro* and *in vivo*. *J. Infect. Dis.* *208*, 1553–1560.
25. Marín-Menéndez, A., Montis, C., Díaz-Calvo, T., Carta, D., Hatzixanthis, K., Morris, C.J., McArthur, M., and Berti, D. (2017). Antimicrobial Nanoplexes meet Model Bacterial Membranes: the key role of Cardiolipin. *Sci. Rep.* *7*, 41242.
26. Równicki, M., Dąbrowska, Z., Wojciechowska, M., Wierzbka, A.J., Maximova, K., Gryko, D., and Trylska, J. (2019). Inhibition of *Escherichia coli* Growth by Vitamin B12–Peptide Nucleic Acid Conjugates. *ACS Omega* *4*, 819–824.
27. Zhang, Y., Xie, X., Ma, W., Zhan, Y., Mao, C., Shao, X., and Lin, Y. (2020). Multi-targeted Antisense Oligonucleotide Delivery by a Framework Nucleic Acid for Inhibiting Biofilm Formation and Virulence. *Nano-Micro Lett.* *12*, 74.
28. Rahman, M.A., Summerton, J., Foster, E., Cunningham, K., Stirchak, E., Weller, D., and Schaup, H.W. (1991). Antibacterial activity and inhibition of protein synthesis in *Escherichia coli* by antisense DNA analogs. *Antisense Res. Dev.* *1*, 319–327.
29. Nekhotiaeva, N., Awasthi, S.K., Nielsen, P.E., and Good, L. (2004). Inhibition of *Staphylococcus aureus* gene expression and growth using antisense peptide nucleic acids. *Mol. Ther.* *10*, 652–659.
30. Patenge, N., Pappesch, R., Krawack, F., Walda, C., Mraheil, M.A., Jacob, A., Hain, T., and Kreikemeyer, B. (2013). Inhibition of Growth and Gene Expression by PNA-peptide Conjugates in *Streptococcus pyogenes*. *Mol. Ther. Nucleic Acids* *2*, e132.
31. Kurupati, P., Tan, K.S.W., Kumarasinghe, G., and Poh, C.L. (2007). Inhibition of gene expression and growth by antisense peptide nucleic acids in a multiresistant beta-lactamase-producing *Klebsiella pneumoniae* strain. *Antimicrob. Agents Chemother.* *51*, 805–811.
32. Wang, H., He, Y., Xia, Y., Wang, L., and Liang, S. (2014). Inhibition of gene expression and growth of multidrug-resistant *Acinetobacter baumannii* by antisense peptide nucleic acids. *Mol. Biol. Rep.* *41*, 7535–7541.
33. Rajasekaran, P., Alexander, J.C., Seleem, M.N., Jain, N., Sriranganathan, N., Wattam, A.R., Setubal, J.C., and Boyle, S.M. (2013). Peptide nucleic acids inhibit growth of *Brucella suis* in pure culture and in infected murine macrophages. *Int. J. Antimicrob. Agents* *41*, 358–362.
34. Good, L., Awasthi, S.K., Dryselius, R., Larsson, O., and Nielsen, P.E. (2001). Bactericidal antisense effects of peptide–PNA conjugates. *Nat. Biotechnol.* *19*, 360–364.
35. Ghosal, A., and Nielsen, P.E. (2012). Potent Antibacterial Antisense Peptide–Peptide Nucleic Acid Conjugates Against *Pseudomonas aeruginosa*. *Nucleic Acid Therapeut.* *22*, 323–334.
36. Barkowsky, G., Lemser, A.L., Pappesch, R., Jacob, A., Krüger, S., Schröder, A., Kreikemeyer, B., and Patenge, N. (2019). Influence of Different Cell-Penetrating Peptides on the Antimicrobial Efficiency of PNAs in *Streptococcus pyogenes*. *Mol. Ther. Nucleic Acids* *18*, 444–454.
37. Zhang, Y., Ma, W., Zhu, Y., Shi, S., Li, Q., Mao, C., Zhao, D., Zhan, Y., Shi, J., Li, W., et al. (2018). Inhibiting Methicillin-Resistant *Staphylococcus aureus* by Tetrahedral DNA Nanostructure-enabled Antisense Peptide Nucleic Acid Delivery. *Nano Lett.* *18*, 5652–5659.
38. Meng, J., Da, F., Ma, X., Wang, N., Wang, Y., Zhang, H., Li, M., Zhou, Y., Xue, X., Hou, Z., et al. (2015). Antisense growth inhibition of methicillin-resistant *Staphylococcus aureus* by locked nucleic acid conjugated with cell-penetrating peptide as a novel FtsZ inhibitor. *Antimicrob. Agents Chemother.* *59*, 914–922.
39. Yavari, N., Goltermann, L., and Nielsen, P.E. (2021). Uptake, Stability, and Activity of Antisense Anti-*acpP* PNA–Peptide Conjugates in *Escherichia coli* and the Role of SbmA. *ACS Chem. Biol.* *16*, 471–479.
40. Tilley, L.D., Hine, O.S., Kellogg, J.A., Hassinger, J.N., Weller, D.D., Iversen, P.L., and Geller, B.L. (2006). Gene-specific effects of antisense phosphorodiamidate morpholino oligomer–peptide conjugates on *Escherichia coli* and *Salmonella enterica* serovar typhimurium in pure culture and in tissue culture. *Antimicrob. Agents Chemother.* *50*, 2789–2796.
41. Mellbye, B.L., Puckett, S.E., Tilley, L.D., Iversen, P.L., and Geller, B.L. (2009). Variations in amino acid composition of antisense peptide-phosphorodiamidate morpholino oligomer affect potency against *Escherichia coli* *in vitro* and *in vivo*. *Antimicrob. Agents Chemother.* *53*, 525–530.
42. Perche, F., Le Gall, T., Montier, T., Pichon, C., and Malinge, J.M. (2019). Cardiolipin-Based Lipopolyplex Platform for the Delivery of Diverse Nucleic Acids into Gram-Negative Bacteria. *Pharmaceuticals* *12*, 81.
43. Narenji, H., Teymournejad, O., Rezaee, M.A., Taghizadeh, S., Mehrmuz, B., Aghazadeh, M., Asgharzadeh, M., Madhi, M., Gholizadeh, P., Ganbarov, K., et al. (2020). Antisense peptide nucleic acids against *ftsZ* and *efaA* genes inhibit growth and biofilm formation of *Enterococcus faecalis*. *Microb. Pathog.* *139*, 103907.
44. Dryselius, R., Nekhotiaeva, N., and Good, L. (2005). Antimicrobial synergy between mRNA- and protein-level inhibitors. *J. Antimicrob. Chemother.* *56*, 97–103.
45. Hegarty, J.P., and Stewart, D.B., Sr. (2018). Advances in therapeutic bacterial antisense biotechnology. *Appl. Microbiol. Biotechnol.* *102*, 1055–1065.
46. White, D.G., Maneewannakul, K., von Hofe, E., Zillman, M., Eisenberg, W., Field, A.K., and Levy, S.B. (1997). Inhibition of the Multiple Antibiotic Resistance (mar) Operon in *Escherichia coli* by Antisense DNA Analogs. *Antimicrob. Agents Chemother.* *41*, 2699–2704.
47. Sharma, P., Haycocks, J.R.J., Middlemiss, A.D., Kettles, R.A., Sellars, L.E., Ricci, V., Piddock, L.J.V., and Grainger, D.C. (2017). The multiple antibiotic resistance operon of enteric bacteria controls DNA repair and outer membrane integrity. *Nat. Commun.* *8*, 1444.
48. Oh, E., Zhang, Q., and Jeon, B. (2014). Target optimization for peptide nucleic acid (PNA)-mediated antisense inhibition of the CmeABC multidrug efflux pump in *Campylobacter jejuni*. *J. Antimicrob. Chemother.* *69*, 375–380.
49. Wang, H., Meng, J., Jia, M., Ma, X., He, G., Yu, J., Wang, R., Bai, H., Hou, Z., and Luo, X. (2010). *oprM* as a new target for reversion of multidrug resistance in *Pseudomonas aeruginosa* by antisense phosphorothioate oligodeoxynucleotides. *FEMS Immunol. Med. Microbiol.* *60*, 275–282.
50. Meng, J., Bai, H., Jia, M., Ma, X., Hou, Z., Xue, X., Zhou, Y., and Luo, X. (2012). Restoration of antibiotic susceptibility in fluoroquinolone-resistant *Escherichia coli* by targeting *acrB* with antisense phosphorothioate oligonucleotide encapsulated in novel anion liposome. *J. Antibiot.* *65*, 129–134.
51. Goh, S., Loeffler, A., Lloyd, D.H., Nair, S.P., and Good, L. (2015). Oxacillin sensitization of methicillin-resistant *Staphylococcus aureus* and methicillin-resistant *Staphylococcus pseudintermedius* by antisense peptide nucleic acids *in vitro*. *BMC Microbiol.* *15*, 262.
52. Skvortsova, Y.V., Salina, E.G., Burakova, E.A., Bychenko, O.S., Stetsenko, D.A., and Azhikina, T.L. (2019). A New Antisense Phosphoryl Guanidine Oligo-2'-OMethylribonucleotide Penetrates Into Intracellular Mycobacteria and Suppresses Target Gene Expression. *Front. Pharmacol.* *10*, 1049.
53. Wahlestedt, C., Salmi, P., Good, L., Kela, J., Johnsson, T., Hökfelt, T., Broberger, C., Porreca, F., Lai, J., Ren, K., et al. (2000). Potent and nontoxic antisense oligonucleotides containing locked nucleic acids. *Proc. Natl. Acad. Sci. USA* *97*, 5633–5638.
54. Fedoroff, O.Y., Salazar, M., and Reid, B.R. (1993). Structure of a DNA : RNA Hybrid Duplex: Why RNase H Does Not Cleave Pure RNA. *J. Mol. Biol.* *233*, 509–523.
55. Minasov, G., Teplova, M., Nielsen, P., Wengel, J., and Egli, M. (2000). Structural basis of cleavage by RNase H of hybrids of arabinonucleic acids and RNA. *Biochemistry* *39*, 3525–3532.
56. Bai, H., Xue, X., Hou, Z., Zhou, Y., Meng, J., and Luo, X. (2010). Antisense Antibiotics: A Brief Review of Novel Target Discovery and Delivery. *Curr. Drug Discov. Technol.* *7*, 76–85.
57. Bennett, C.F., and Swayze, E.E. (2010). RNA targeting therapeutics: molecular mechanisms of antisense oligonucleotides as a therapeutic platform. *Annu. Rev. Pharmacol. Toxicol.* *50*, 259–293.
58. Petersen, M., and Wengel, J. (2003). LNA: a versatile tool for therapeutics and genomics. *Trends Biotechnol.* *21*, 74–81.
59. Kurreck, J., Wyszko, E., Gillen, C., and Erdmann, V.A. (2002). Design of antisense oligonucleotides stabilized by locked nucleic acids. *Nucleic Acids Res.* *30*, 1911–1918.
60. Burel, S.A., Hart, C.E., Cauntay, P., Hsiao, J., Macheimer, T., Katz, M., Watt, A., Bui, H.H., Younis, H., Sabripour, M., et al. (2016). Hepatotoxicity of high affinity gapmer antisense oligonucleotides is mediated by RNase H1 dependent promiscuous reduction of very long pre-mRNA transcripts. *Nucleic Acids Res.* *44*, 2093–2109.

61. Kasuya, T., Hori, S.I., Watanabe, A., Nakajima, M., Gahara, Y., Rokushima, M., Yanagimoto, T., and Kugimiya, A. (2016). Ribonuclease H1-dependent hepatotoxicity caused by locked nucleic acid-modified gapmer antisense oligonucleotides. *Sci. Rep.* 6, 30377.
62. Dieckmann, A., Hagedorn, P.H., Burki, Y., Brüggmann, C., Berrera, M., Ebeling, M., Singer, T., and Schuler, F. (2018). A Sensitive *In Vitro* Approach to Assess the Hybridization-Dependent Toxic Potential of High Affinity Gapmer Oligonucleotides. *Mol. Ther. Nucleic Acids* 10, 45–54.
63. Dryselius, R., Aswasti, S.K., Rajarao, G.K., Nielsen, P.E., and Good, L. (2003). The translation start codon region is sensitive to antisense PNA inhibition in *Escherichia coli*. *Oligonucleotides* 13, 427–433.
64. Sully, E.K., and Geller, B.L. (2016). Antisense antimicrobial therapeutics. *Curr. Opin. Microbiol.* 33, 47–55.
65. Summerton, J., Stein, D., Huang, S.B., Matthews, P., Weller, D., and Partridge, M. (1997). Morpholino and Phosphorothioate Antisense Oligomers Compared in Cell-Free and In-Cell Systems. *Antisense Nucleic Acid Drug Dev.* 7, 63–70.
66. Kulkarni, J.A., Witzigmann, D., Thomson, S.B., Chen, S., Leavitt, B.R., Cullis, P.R., and van der Meel, R. (2021). The current landscape of nucleic acid therapeutics. *Nat. Nanotechnol.* 16, 630–643.
67. Brown, S.C., Thomson, S.A., Veal, J.M., and Davis, D.G. (1994). NMR Solution Structure of a Peptide Nucleic Acid Complexed with RNA. *Science* 265, 777–780.
68. Shi, N., Boado, R.J., and Pardridge, W.M. (2000). Antisense imaging of gene expression in the brain *in vivo*. *Proc. Natl. Acad. Sci. USA* 97, 14709–14714.
69. Suzuki, T., Wu, D., Schlachetzki, F., Li, J.Y., Boado, R.J., and Pardridge, W.M. (2004). Imaging Endogenous Gene Expression in Brain Cancer *In Vivo* with ¹¹¹In-Peptide Nucleic Acid Antisense Radiopharmaceuticals and Brain Drug-Targeting Technology. *J. Nucl. Med.* 45, 1766–1775.
70. Sahu, B., Sacui, I., Rapireddy, S., Zanolli, K.J., Bahal, R., Armitage, B.A., and Ly, D.H. (2011). Synthesis and characterization of conformationally preorganized, (R)-diethylene glycol-containing gamma-peptide nucleic acids with superior hybridization properties and water solubility. *J. Org. Chem.* 76, 5614–5627.
71. Moreira, L., Guimarães, N.M., Pereira, S., Santos, R.S., Loureiro, J.A., Ferreira, R.M., Figueiredo, C., Pereira, M.C., and Azevedo, N.F. (2023). Engineered liposomes to deliver nucleic acid mimics in *Escherichia coli*. *J. Contr. Release* 355, 489–500.
72. Moreira, L., Guimarães, N.M., Pereira, S., Santos, R.S., Loureiro, J.A., Pereira, M.C., and Azevedo, N.F. (2022). Liposome Delivery of Nucleic Acids in Bacteria: Toward *In Vivo* Labeling of Human Microbiota. *ACS Infect. Dis.* 8, 1218–1230.
73. Pereira, S., Yao, R., Gomes, M., Jørgensen, P.T., Wengel, J., Azevedo, N.F., and Sobral Santos, R. (2021). Can Vitamin B12 Assist the Internalization of Antisense LNA Oligonucleotides into Bacteria? *Antibiotics* 10, 379.
74. Santos, R.S., Dakwar, G.R., Zagato, E., Brans, T., Figueiredo, C., Raemdonck, K., Azevedo, N.F., De Smedt, S.C., and Braeckmans, K. (2017). Intracellular delivery of oligonucleotides in *Helicobacter pylori* by fusogenic liposomes in the presence of gastric mucus. *Biomaterials* 138, 1–12.
75. Wengel, J. (1999). Synthesis of 3'-C- and 4'-C-Branched Oligodeoxynucleotides and the Development of Locked Nucleic Acid (LNA). *Acc. Chem. Res.* 32, 301–310.
76. Egli, M., and Manoharan, M. (2023). Chemistry, structure and function of approved oligonucleotide therapeutics. *Nucleic Acids Res.* 51, 2529–2573.
77. Molenaar, C., Marras, S.A., Slats, J.C., Truffert, J.C., Lemaître, M., Raap, A.K., Dirks, R.W., and Tanke, H.J. (2001). Linear 2' O-Methyl RNA probes for the visualization of RNA in living cells. *Nucleic Acids Res.* 29, E89.
78. Yang, C.J., Wang, L., Wu, Y., Kim, Y., Medley, C.D., Lin, H., and Tan, W. (2007). Synthesis and investigation of deoxyribonucleic acid/locked nucleic acid chimeric molecular beacons. *Nucleic Acids Res.* 35, 4030–4041.
79. Obika, S., Nanbu, D., Hari, Y., Andoh, J.I., Morio, K.I., Doi, T., and Imanishi, T. (1998). Stability and structural features of the duplexes containing nucleoside analogues with a fixed N-type conformation, 2'-O,4'-C-methyleneribonucleosides. *Tetrahedron Lett.* 39, 5401–5404.
80. Koshkin, A.A., Singh, S.K., Nielsen, P., Rajwansi, V.K., Kumar, R., Meldgaard, M., Olsen, C.E., and Wengel, J. (1998). LNA (Locked Nucleic Acids): Synthesis of the adenine, cytosine, guanine, 5-methylcytosine, thymine and uracil bicyclonucleoside monomers, oligomerisation, and unprecedented nucleic acid recognition. *Tetrahedron* 54, 3607–3630.
81. Bai, H., Sang, G., You, Y., Xue, X., Zhou, Y., Hou, Z., Meng, J., and Luo, X. (2012). Targeting RNA polymerase primary sigma70 as a therapeutic strategy against methicillin-resistant *Staphylococcus aureus* by antisense peptide nucleic acid. *PLoS One* 7, e29886.
82. Tan, X.X., Actor, J.K., and Chen, Y. (2005). Peptide nucleic acid antisense oligomer as a therapeutic strategy against bacterial infection: proof of principle using mouse intraperitoneal infection. *Antimicrob. Agents Chemother.* 49, 3203–3207.
83. Alajlouni, R.A., and Seleem, M.N. (2013). Targeting *Listeria Monocytogenes* rpoA and rpoD Genes Using Peptide Nucleic Acids. *Nucleic Acid Therapeut.* 23, 363–367.
84. Maekawa, K., Azuma, M., Okuno, Y., Tsukamoto, T., Nishiguchi, K., Setsukinai, K.I., Maki, H., Numata, Y., Takemoto, H., and Rokushima, M. (2015). Antisense peptide nucleic acid-peptide conjugates for functional analyses of genes in *Pseudomonas aeruginosa*. *Bioorg. Med. Chem.* 23, 7234–7239.
85. Hegarty, J.P., Krzeminski, J., Sharma, A.K., Guzman-Villanueva, D., Weissig, V., and Stewart, D.B., Sr. (2016). Bolaamphiphile-based nanocomplex delivery of phosphorothioate gapmer antisense oligonucleotides as a treatment for *Clostridium difficile*. *Int. J. Nanomed.* 11, 3607–3619.
86. Giedyk, M., Jackowska, A., Równicki, M., Kolanowska, M., Trylska, J., and Gryko, D. (2019). Vitamin B12 transports modified RNA into *E. coli* and *S. Typhimurium* cells. *Chem. Commun.* 55, 763–766.
87. Hibbitts, A., Lucía, A., Serrano-Sevilla, I., De Matteis, L., McArthur, M., de la Fuente, J.M., Ainsa, J.A., and Navarro, F. (2019). Co-delivery of free vancomycin and transcription factor decoy-nanostructured lipid carriers can enhance inhibition of methicillin resistant *Staphylococcus aureus* (MRSA). *PLoS One* 14, e0220684.
88. Good, L., Sandberg, R., Larsson, O., Nielsen, P.E., and Wahlestedt, C. (2000). Antisense PNA effects in *Escherichia coli* are limited by the outer-membrane LPS layer. *Microbiology* 146, 2665–2670.
89. Eriksson, M., Nielsen, P.E., and Good, L. (2002). Cell permeabilization and uptake of antisense peptide-peptide nucleic acid (PNA) into *Escherichia coli*. *J. Biol. Chem.* 277, 7144–7147.
90. Santos, R.S., Guimarães, N., Madureira, P., and Azevedo, N.F. (2014). Optimization of a peptide nucleic acid fluorescence *in situ* hybridization (PNA-FISH) method for the detection of bacteria and disclosure of a formamide effect. *J. Biotechnol.* 187, 16–24.
91. Traglia, G.M., Sala, C.D., Fuxman Bass, J.I., Soler-Bistué, A.J.C., Zorreguieta, A., Ramirez, M.S., and Tolmasey, M.E. (2012). Internalization of Locked Nucleic Acids/DNA Hybrid Oligomers into *Escherichia coli*. *Biores. Open Access* 1, 260–263.
92. Santos, R.S., Figueiredo, C., Azevedo, N.F., Braeckmans, K., and De Smedt, S.C. (2018). Nanomaterials and molecular transporters to overcome the bacterial envelope barrier: Towards advanced delivery of antibiotics. *Adv. Drug Deliv. Rev.* 136–137, 28–48.
93. Goltermann, L., Yavari, N., Zhang, M., Ghosal, A., and Nielsen, P.E. (2019). PNA Length Restriction of Antibacterial Activity of Peptide-PNA Conjugates in *Escherichia coli* Through Effects of the Inner Membrane. *Front. Microbiol.* 10, 1032.
94. Lopez, C., Arivett, B.A., Actis, L.A., and Tolmasey, M.E. (2015). Inhibition of AAC(6)-Ib-mediated resistance to amikacin in *Acinetobacter baumannii* by an antisense peptide-conjugated 2',4'-bridged nucleic acid-NC-DNA hybrid oligomer. *Antimicrob. Agents Chemother.* 59, 5798–5803.
95. Abushahba, M.F.N., Mohammad, H., Thangamani, S., Hussein, A.A.A., and Seleem, M.N. (2016). Impact of different cell penetrating peptides on the efficacy of antisense therapeutics for targeting intracellular pathogens. *Sci. Rep.* 6, 20832.
96. Geller, B.L., Deere, J.D., Stein, D.A., Kroeker, A.D., Moulton, H.M., and Iversen, P.L. (2003). Inhibition of gene expression in *Escherichia coli* by antisense phosphorodiamidate morpholino oligomers. *Antimicrob. Agents Chemother.* 47, 3233–3239.
97. Kulyté, A., Nekhotiaeva, N., Awasthi, S.K., and Good, L. (2005). Inhibition of *Mycobacterium smegmatis* gene expression and growth using antisense peptide nucleic acids. *J. Mol. Microbiol. Biotechnol.* 9, 101–109.

98. Ghosal, A., Vitali, A., Stach, J.E.M., and Nielsen, P.E. (2013). Role of SbmA in the uptake of peptide nucleic acid (PNA)-peptide conjugates in *E. coli*. *ACS Chem. Biol.* *8*, 360–367.
99. Amantana, A., Moulton, H.M., Cate, M.L., Reddy, M.T., Whitehead, T., Hassinger, J.N., Youngblood, D.S., and Iversen, P.L. (2007). Pharmacokinetics, Biodistribution, Stability and Toxicity of a Cell-Penetrating Peptide-Morpholino Oligomer Conjugate. *Bioconjugate Chem.* *18*, 1325–1331.
100. Tilley, L.D., Mellbye, B.L., Puckett, S.E., Iversen, P.L., and Geller, B.L. (2007). Antisense peptide-phosphorodiamidate morpholino oligomer conjugate: dose-response in mice infected with *Escherichia coli*. *J. Antimicrob. Chemother.* *59*, 66–73.
101. Vaara, M., and Porro, M. (1996). Group of Peptides That Act Synergistically with Hydrophobic Antibiotics against Gram-Negative Enteric Bacteria. *Antimicrob. Agents Chemother.* *40*, 1801–1805.
102. Barkowsky, G., Abt, C., Pöhner, I., Bieda, A., Hammerschmidt, S., Jacob, A., Kreikemeyer, B., and Patenge, N. (2022). Antimicrobial Activity of Peptide-Coupled Antisense Peptide Nucleic Acids in *Streptococcus pneumoniae*. *Microbiol. Spectr.* *10*, e0049722.
103. Martínez-Gutián, M., Vázquez-Ucha, J.C., Álvarez-Fraga, L., Conde-Pérez, K., Bou, G., Poza, M., and Beceiro, A. (2020). Antisense inhibition of *lpxB* gene expression in *Acinetobacter baumannii* by peptide-PNA conjugates and synergy with colistin. *J. Antimicrob. Chemother.* *75*, 51–59.
104. El-Andaloussi, S., Järver, P., Johansson, H.J., and Langel, U. (2007). Cargo-dependent cytotoxicity and delivery efficacy of cell-penetrating peptides: a comparative study. *Biochem. J.* *407*, 285–292.
105. Lupfer, C., Stein, D.A., Mourich, D.V., Tepper, S.E., Iversen, P.L., and Pastey, M. (2008). Inhibition of influenza A H3N8 virus infections in mice by morpholino oligomers. *Arch. Virol.* *153*, 929–937.
106. Abes, S., Moulton, H.M., Clair, P., Prevot, P., Youngblood, D.S., Wu, R.P., Iversen, P.L., and Lebleu, B. (2006). Vectorization of morpholino oligomers by the (R-Ahx-R)4 peptide allows efficient splicing correction in the absence of endosomolytic agents. *J. Contr. Release* *116*, 304–313.
107. Youngblood, D.S., Hatlevig, S.A., Hassinger, J.N., Iversen, P.L., and Moulton, H.M. (2007). Stability of Cell-Penetrating Peptide-Morpholino Oligomer Conjugates in Human Serum and in Cells. *Bioconjugate Chem.* *18*, 50–60.
108. Iubatti, M., Gabas, I.M., Cavaco, L.M., Mood, E.H., Lim, E., Bonanno, F., Yavari, N., Brolin, C., and Nielsen, P.E. (2022). Antisense Peptide Nucleic Acid-Diaminobutanoic Acid Dendron Conjugates with SbmA-Independent Antimicrobial Activity against Gram-Negative Bacteria. *ACS Infect. Dis.* *8*, 1098–1106.
109. Li, J., Pei, H., Zhu, B., Liang, L., Wei, M., He, Y., Chen, N., Li, D., Huang, Q., and Fan, C. (2011). Self-Assembled Multivalent DNA Nanostructures for Noninvasive Intracellular Delivery of Immunostimulatory CpG Oligonucleotides. *ACS Nano* *5*, 8783–8789.
110. Lee, H., Lytton-Jean, A.K.R., Chen, Y., Love, K.T., Park, A.I., Karagiannis, E.D., Sehgal, A., Querbes, W., Zurenko, C.S., Jayaraman, M., et al. (2012). Molecularly self-assembled nucleic acid nanoparticles for targeted *in vivo* siRNA delivery. *Nat. Nanotechnol.* *7*, 389–393.
111. Huang, Y., Huang, W., Chan, L., Zhou, B., and Chen, T. (2016). A multifunctional DNA origami as carrier of metal complexes to achieve enhanced tumoral delivery and nullified systemic toxicity. *Biomaterials* *103*, 183–196.
112. Readman, J.B., Dickson, G., and Coldham, N.G. (2017). Tetrahedral DNA Nanoparticle Vector for Intracellular Delivery of Targeted Peptide Nucleic Acid Antisense Agents to Restore Antibiotic Sensitivity in Cefotaxime-Resistant *Escherichia coli*. *Nucleic Acid Therapeut.* *27*, 176–181.
113. Hu, Y., Chen, Z., Mao, X., Li, M., Hou, Z., Meng, J., Luo, X., and Xue, X. (2020). Loop-armed DNA tetrahedron nanoparticles for delivering antisense oligos into bacteria. *J. Nanobiotechnol.* *18*, 109.
114. Setyawati, M.I., Kutty, R.V., Tay, C.Y., Yuan, X., Xie, J., and Leong, D.T. (2014). Novel theranostic DNA nanoscaffolds for the simultaneous detection and killing of *Escherichia coli* and *Staphylococcus aureus*. *ACS Appl. Mater. Interfaces* *6*, 21822–21831.
115. Sun, Y., Liu, Y., Zhang, B., Shi, S., Zhang, T., Zhao, D., Tian, T., Li, Q., and Lin, Y. (2021). Erythromycin loaded by tetrahedral framework nucleic acids are more antimicrobial sensitive against *Escherichia coli* (*E. coli*). *Bioact. Mater.* *6*, 2281–2290.
116. Liu, M., Chu, B., Sun, R., Ding, J., Ye, H., Yang, Y., Wu, Y., Shi, H., Song, B., He, Y., et al. (2023). Antisense Oligonucleotides Selectively Enter Human-Derived Antibiotic-Resistant Bacteria through Bacterial-Specific ATP-Binding Cassette Sugar Transporter. *Adv. Mater.* *35*, e2300477.
117. Fillion, P., Desjardins, A., Sayasith, K., and Lagacé, J. (2001). Encapsulation of DNA in negatively charged liposomes and inhibition of bacterial gene expression with fluid liposome-encapsulated antisense oligonucleotides. *Biochim. Biophys. Acta* *1515*, 44–54.
118. Kauss, T., Arpin, C., Bientz, L., Vinh Nguyen, P., Violet, B., Benizri, S., and Barthélémy, P. (2020). Lipid oligonucleotides as a new strategy for tackling the antibiotic resistance. *Sci. Rep.* *10*, 1054.
119. Long, Q., Jia, B., Shi, Y., Wang, Q., Yu, H., and Li, Z. (2021). DNA Nanodevice as a Co-delivery Vehicle of Antisense Oligonucleotide and Silver Ions for Selective Inhibition of Bacteria Growth. *ACS Appl. Mater. Interfaces* *13*, 47987–47995.
120. Pasquina-Lemonche, L., Burns, J., Turner, R.D., Kumar, S., Tank, R., Mullin, N., Wilson, J.S., Chakrabarti, B., Bullough, P.A., Foster, S.J., and Hobbs, J.K. (2020). The architecture of the Gram-positive bacterial cell wall. *Nature* *582*, 294–297.
121. Da, F., Yao, L., Su, Z., Hou, Z., Li, Z., Xue, X., Meng, J., and Luo, X. (2017). Antisense locked nucleic acids targeting *agrA* inhibit quorum sensing and pathogenesis of community-associated methicillin-resistant *Staphylococcus aureus*. *J. Appl. Microbiol.* *122*, 257–267.
122. Traykovska, M., Otcheva, L.A., and Penchovsky, R. (2022). Targeting TPP Riboswitches Using Chimeric Antisense Oligonucleotide Technology for Antibacterial Drug Development. *ACS Appl. Bio Mater.* *5*, 4896–4902.
123. Traykovska, M., and Penchovsky, R. (2022). Targeting SAM-I Riboswitch Using Antisense Oligonucleotide Technology for Inhibiting the Growth of *Staphylococcus aureus* and *Listeria monocytogenes*. *Antibiotics* *11*, 1662.
124. Chen, Z., Hu, Y., Mao, X., Nie, D., Zhao, H., Hou, Z., Li, M., Meng, J., Luo, X., and Xue, X. (2022). Amphipathic dendritic poly-peptides carrier to deliver antisense oligonucleotides against multi-drug resistant bacteria *in vitro* and *in vivo*. *J. Nanobiotechnol.* *20*, 180.
125. Harth, G., Zamecnik, P.C., Tabatadze, D., Pierson, K., and Horwitz, M.A. (2007). Hairpin extensions enhance the efficacy of mycolyl transferase-specific antisense oligonucleotides targeting *Mycobacterium tuberculosis*. *Proc. Natl. Acad. Sci. USA* *104*, 7199–7204.
126. Wu, S., Gan, T., Xie, L., Deng, S., Liu, Y., Zhang, H., Hu, X., and Lei, L. (2022). Antibacterial performance of graphene oxide/alginate-based antisense hydrogel for potential therapeutic application in *Staphylococcus aureus* infection. *Biomater. Adv.* *141*, 213121.
127. Wu, S., Liu, Y., Zhang, H., and Lei, L. (2020). Nano-graphene oxide with antisense *walR* RNA inhibits the pathogenicity of *Enterococcus faecalis* in periapical periodontitis. *J. Dent. Sci.* *15*, 65–74.
128. Duan, G., Zhang, Y., Luan, B., Weber, J.K., Zhou, R.W., Yang, Z., Zhao, L., Xu, J., Luo, J., and Zhou, R. (2017). Graphene-Induced Pore Formation on Cell Membranes. *Sci. Rep.* *7*, 42767.
129. Beha, M.J., Ryu, J.S., Kim, Y.S., and Chung, H.J. (2021). Delivery of antisense oligonucleotides using multi-layer coated gold nanoparticles to methicillin-resistant *S. aureus* for combinatorial treatment. *Mater. Sci. Eng. C* *126*, 112167.
130. Zhang, Y., Lai, L., Liu, Y., Chen, B., Yao, J., Zheng, P., Pan, Q., and Zhu, W. (2022). Biomimetic Cascade Enzyme-Encapsulated ZIF-8 Nanoparticles Combined with Antisense Oligonucleotides for Drug-Resistant Bacteria Treatment. *ACS Appl. Mater. Interfaces* *14*, 6453–6464.
131. McArthur, M., and Bibb, M.J. (2008). Manipulating and understanding antibiotic production in *Streptomyces coelicolor* A3(2) with decoy oligonucleotides. *Proc. Natl. Acad. Sci. USA* *105*, 1020–1025.
132. Wang, B., Guo, F., Dong, S.H., and Zhao, H. (2019). Activation of silent biosynthetic gene clusters using transcription factor decoys. *Nat. Chem. Biol.* *15*, 111–114.

133. Wang, T., Tague, N., Whelan, S.A., and Dunlop, M.J. (2021). Programmable gene regulation for metabolic engineering using decoy transcription factor binding sites. *Nucleic Acids Res.* *49*, 1163–1172.
134. González-Paredes, A., Sitia, L., Ruyra, A., Morris, C.J., Wheeler, G.N., McArthur, M., and Gasco, P. (2019). Solid lipid nanoparticles for the delivery of anti-microbial oligonucleotides. *Eur. J. Pharm. Biopharm.* *134*, 166–177.
135. Crinelli, R., Bianchi, M., Gentilini, L., and Magnani, M. (2002). Design and characterization of decoy oligonucleotides containing locked nucleic acids. *Nucleic Acids Res.* *30*, 2435–2443.
136. Bielinska, A., Shivdasani, R.A., Zhang, L.Q., and Nabel, G.J. (1990). Regulation of Gene Expression with Double-Stranded Phosphorothioate Oligonucleotides. *Science* *250*, 997–1000.
137. Wee, J.H., Zhang, Y.L., Rhee, C.S., and Kim, D.Y. (2017). Inhibition of Allergic Response by Intranasal Selective NF-kappaB Decoy Oligodeoxynucleotides in a Murine Model of Allergic Rhinitis. *Allergy Asthma Immunol. Res.* *9*, 61–69.
138. Romanelli, A., Pedone, C., Saviano, M., Bianchi, N., Borgatti, M., Mischiati, C., and Gambari, R. (2001). Molecular interactions with nuclear factor kappaB (NF-kappaB) transcription factors of a PNA-DNA chimera mimicking NF-kappaB binding sites. *Eur. J. Biochem.* *268*, 6066–6075.
139. Borgatti, M., Lampronti, I., Romanelli, A., Pedone, C., Saviano, M., Bianchi, N., Mischiati, C., and Gambari, R. (2003). Transcription factor decoy molecules based on a peptide nucleic acid (PNA)-DNA chimera mimicking Sp1 binding sites. *J. Biol. Chem.* *278*, 7500–7509.
140. Crinelli, R., Bianchi, M., Gentilini, L., Palma, L., Sørensen, M.D., Bryld, T., Babu, R.B., Arar, K., Wengel, J., and Magnani, M. (2004). Transcription factor decoy oligonucleotides modified with locked nucleic acids: an *in vitro* study to reconcile biostability with binding affinity. *Nucleic Acids Res.* *32*, 1874–1885.
141. Dubrac, S., Boneca, I.G., Poupel, O., and Msadek, T. (2007). New insights into the WalK/WalR (YycG/YycF) essential signal transduction pathway reveal a major role in controlling cell wall metabolism and biofilm formation in *Staphylococcus aureus*. *J. Bacteriol.* *189*, 8257–8269.
142. Howden, B.P., McEvoy, C.R.E., Allen, D.L., Chua, K., Gao, W., Harrison, P.F., Bell, J., Coombs, G., Bennett-Wood, V., Porter, J.L., et al. (2011). Evolution of Multidrug Resistance during *Staphylococcus aureus* Infection Involves Mutation of the Essential Two Component Regulator WalKR. *PLoS Pathog.* *7*, e1002359.
143. Fokina, A.A., Stetsenko, D.A., and François, J.C. (2015). DNA enzymes as potential therapeutics: towards clinical application of 10-23 DNazymes. *Expert Opin. Biol. Ther.* *15*, 689–711.
144. Hou, Z., Meng, J.R., Zhao, J.R., Hu, B.Q., Liu, J., Yan, X.J., Jia, M., and Luo, X.X. (2007). Inhibition of beta-lactamase-mediated oxacillin resistance in *Staphylococcus aureus* by a deoxyribozyme. *Acta Pharmacol. Sin.* *28*, 1775–1782.
145. Chen, F., Li, Z., Wang, R., Liu, B., Zeng, Z., Zhang, H., and Zhang, J. (2004). Inhibition of Ampicillin-Resistant Bacteria by Novel Mono-DNazymes and Di-DNAzyme Targeted to B-Lactamase mRNA. *Oligonucleotides* *14*, 80–89.
146. Hou, Z., Meng, J.R., Niu, C., Wang, H.F., Liu, J., Hu, B.Q., Jia, M., and Luo, X.X. (2007). Restoration of antibiotic susceptibility in methicillin-resistant *Staphylococcus aureus* by targeting *mecR1* with a phosphorothioate deoxyribozyme. *Clin. Exp. Pharmacol. Physiol.* *34*, 1160–1164.
147. Hou, Z., Zhou, Y., Wang, H., Bai, H., Meng, J., Xue, X., and Luo, X. (2011). Co-blockade of *mecR1*/*blaR1* signal pathway to restore antibiotic susceptibility in clinical isolates of methicillin-resistant *Staphylococcus aureus*. *Arch. Med. Sci.* *7*, 414–422.
148. Li, J., Zhu, D., Yi, Z., He, Y., Chun, Y., Liu, Y., and Li, N. (2005). DNazymes Targeting the *icl* Gene Inhibit ICL Expression and Decrease *Mycobacterium tuberculosis* Survival in Macrophages. *Oligonucleotides* *15*, 215–222.
149. Schubert, S., Gül, D.C., Grunert, H.P., Zeichhardt, H., Erdmann, V.A., and Kurreck, J. (2003). RNA cleaving '10-23' DNazymes with enhanced stability and activity. *Nucleic Acids Res.* *31*, 5982–5992.
150. Vester, B., Lundberg, L.B., Sørensen, M.D., Babu, B.R., Douthwaite, S., and Wengel, J. (2002). LNAzymes: Incorporation of LNA-Type Monomers into DNazymes Markedly Increases RNA Cleavage. *J. Am. Chem. Soc.* *124*, 13682–13683.
151. Vester, B., Hansen, L.H., Lundberg, L.B., Babu, B.R., Sørensen, M.D., Wengel, J., and Douthwaite, S. (2006). Locked nucleoside analogues expand the potential of DNazymes to cleave structured RNA targets. *BMC Mol. Biol.* *7*, 19.
152. Fluiter, K., Frieden, M., Vreijling, J., Koch, T., and Baas, F. (2005). Evaluation of LNA-modified DNazymes targeting a single nucleotide polymorphism in the large subunit of RNA polymerase II. *Oligonucleotides* *15*, 246–254.
153. Jakobsen, M.R., Haasnoot, J., Wengel, J., Berkhout, B., and Kjems, J. (2007). Efficient inhibition of HIV-1 expression by LNA modified antisense oligonucleotides and DNazymes targeted to functionally selected binding sites. *Retrovirology* *4*, 29.
154. Ran, M., Sun, R., Yan, J., Pulliainen, A.T., Zhang, Y., and Zhang, H. (2023). DNA Nanoflower Eye Drops with Antibiotic-Resistant Gene Regulation Ability for MRSA Keratitis Target Treatment. *Small* *19*, e2304194.
155. Wang, J., Wang, H., Wang, H., He, S., Li, R., Deng, Z., Liu, X., and Wang, F. (2019). Nonviolent Self-Catabolic DNAzyme Nanosponges for Smart Anticancer Drug Delivery. *ACS Nano* *13*, 5852–5863.
156. Wang, J., Yu, S., Wu, Q., Gong, X., He, S., Shang, J., Liu, X., and Wang, F. (2021). A Self-Catabolic Multifunctional DNAzyme Nanosponge for Programmable Drug Delivery and Efficient Gene Silencing. *Angew. Chem.* *60*, 10766–10774.
157. Petinaki, E., Arvaniti, A., Dimitracopoulos, G., and Spiliopoulou, I. (2001). Detection of *mecA*, *mecR1* and *mecI* genes among clinical isolates of methicillin-resistant staphylococci by combined polymerase chain reactions. *J. Antimicrob. Chemother.* *47*, 297–304.
158. Mamusa, M., Sitia, L., Barbero, F., Ruyra, A., Calvo, T.D., Montis, C., Gonzalez-Paredes, A., Wheeler, G.N., Morris, C.J., McArthur, M., and Berti, D. (2017). Cationic liposomal vectors incorporating a bolaamphiphile for oligonucleotide antimicrobials. *Biochim. Biophys. Acta* *1859*, 1767–1777.
159. Lechanteur, A., Furst, T., Evrard, B., Delvenne, P., Hubert, P., and Piel, G. (2016). PEGylation of lipoplexes: The right balance between cytotoxicity and siRNA effectiveness. *Eur. J. Pharmaceut. Sci.* *93*, 493–503.
160. Li, Y., Cui, X.L., Chen, Q.S., Yu, J., Zhang, H., Gao, J., Sun, D.X., and Zhang, G.Q. (2018). Cationic liposomes induce cytotoxicity in HepG2 via regulation of lipid metabolism based on whole-transcriptome sequencing analysis. *BMC Pharmacol. Toxicol.* *19*, 43.
161. Wei, X., Shao, B., He, Z., Ye, T., Luo, M., Sang, Y., Liang, X., Wang, W., Luo, S., Yang, S., et al. (2015). Cationic nanocarriers induce cell necrosis through impairment of Na(+)/K(+)-ATPase and cause subsequent inflammatory response. *Cell Res.* *25*, 237–253.
162. Hattori, Y., Arai, S., Okamoto, R., Hamada, M., Kawano, K., and Yonemochi, E. (2014). Sequential intravenous injection of anionic polymer and cationic lipoplex of siRNA could effectively deliver siRNA to the liver. *Int. J. Pharm.* *476*, 289–298.
163. Hattori, Y., Nakamura, M., Takeuchi, N., Tamaki, K., Shimizu, S., Yoshiike, Y., Taguchi, M., Ohno, H., Ozaki, K.I., and Onishi, H. (2019). Effect of cationic lipid in cationic liposomes on siRNA delivery into the lung by intravenous injection of cationic lipoplex. *J. Drug Target.* *27*, 217–227.
164. Hattori, Y., Tamaki, K., Sakasai, S., Ozaki, K.I., and Onishi, H. (2020). Effects of PEG anchors in PEGylated siRNA lipoplexes on *in vitro* genesilencing effects and siRNA biodistribution in mice. *Mol. Med. Rep.* *22*, 4183–4196.
165. Yoshida, T., Naito, Y., Yasuhara, H., Sasaki, K., Kawaji, H., Kawai, J., Naito, M., Okuda, H., Obika, S., and Inoue, T. (2019). Evaluation of off-target effects of gapmer antisense oligonucleotides using human cells. *Gene Cell.* *24*, 827–835.